Spring 5-1-2010

Investigation of near-infrared fluorescence and photobleaching of human volar side fingertips in vivo: antioxidants and melanin

Colin Wright

Investigation of near-infrared fluorescence and photobleaching of human volar side fingertips *in vivo*: antioxidants and melanin

A Capstone Project Submitted in Partial Fulfillment of the Requirements of the Renée Crown University Honors Program at Syracuse University

Colin Wright

Candidate for B.S. Degree
and Renée Crown University Honors

May 2010

Honors Capstone Project in Biochemistry

Capstone Project Advisor: _____
Joseph Chaiken

Honors Reader: _____
James Dabrowiak

Honors Director: _____
Samuel Gorovitz

Date: _____
April 28, 2010

Abstract

Noninvasive *in vivo* blood glucose determination in the skin of volar side of human fingertips by near-infrared (NIR) Raman spectroscopy relies on fluorescence to quantify blood volume. Fluorescence does not only come from blood, which is composed of plasma and red blood cells; in fact, most fluorescence produced by human fingertips originates in the static tissues, e.g. skin, interstitial fluid, etc.. It will soon be possible to quantify the precise contributions of red blood cells, plasma, and static tissue to the overall fluorescence emission. Observations reveal a systematic decay in fluorescence, which, if not caused by blood movement, challenges our ability to accurately determine blood glucose. In this work, it was found that the fluorescence decay was, in fact, not a result of a blood movement, but instead a chemical change of the static tissues decreasing their fluorescent properties. To identify possible photobleachable material, a series of *in vitro* experiments were performed on various antioxidants and the skin pigment melanin. While none of the antioxidants were found to fluoresce, it was observed that melanin fluoresces, photobleaches, and does not significantly recover its photobleaching. This allows for a deeper understanding as to the chemistry underlying the effect of photobleaching and how it may be accounted for in regards to this technique for glucose measurement.

Table of Contents

Acknowledgments

I would first like to thank Professor Joe Chaiken for his mentorship and constructive feedback during the research and writing processes. I am grateful to Bin Deng for all of her patience and coaching in lab, and to Dr. George Shaheen for his confidence and our discussions at LighTouch. I am very appreciative of the Renée Crown Honors Program for presenting me the opportunity to deeply explore my scientific interests, and for helping me fund my project through the Crown Award. To my parents, Karen and Stephen, thank you for your support in all things that have led me to where I am now.

Introduction

Diabetes mellitus is a disease, characterized by an inability to maintain a healthy glucose concentration because the body either does not produce the hormone insulin (type I) or becomes resistant to it (type II), that affects millions of Americans. Both type I and type II diabetes can cause cardiovascular disease neuropathy, retinopathy (resulting in blindness), end-stage renal disease, foot ulcerations requiring amputation, and death, among other complications. In addition to managing insulin levels, maintaining healthy blood glucose concentration is an essential and often difficult task for every diabetic. The hemoglobin A1C test is performed by physicians to to measure patients' glucose level over long periods of time, but it is also necessary for these patients to self-monitor their glucose concentration, often over a dozen times each day[1].

Most blood glucose meters produce an automatic reading by obtaining a sample of blood, applying it to a reagent strip which is inserted into a reflectance photometer. There are well over twenty meters commercially available, varying in size, weight, and volume of blood drawn; some even allow for blood to be obtained from different parts of the body, such as a finger or forearm[2]. Nevertheless, all of these products require the invasive procedure of piercing the skin to obtain a sample of blood. Given the frequency at which these patients must undergo this painful process to measure their blood glucose concentration, diabetics suffer from scarred and sore fingers, making this chronic disease

extremely unpleasant.

Our system to achieve noninvasive *in vivo* blood and tissue analysis is a key development that has a chance to free diabetics from the pain of managing their disease, as well as to revolutionize many other facets of medicine. A variety of spectroscopic techniques have been investigated including fluorescence spectroscopy, optical rotation, and those using the ultraviolet (UV), near-infrared (NIR) and mid-infrared regions of the spectrum[3]. We rely on the use of near-infrared Raman vibrational spectroscopy to reveal various characteristics of blood, including glucose concentration and hematocrit[4]. The concentration, an amount-per-unit volume of a particular substance, such as glucose, can be readily determined by the analysis of key features of the spectra, namely elastic scattering, inelastic scattering, and fluorescence. While the Raman features (inelastic scattering), which are narrow, are used to determine the relative presence of glucose, and elastic scattering used to monitor red blood cell content, fluorescence, which is relatively broad band, is used to quantify blood volume[5].

We have previously observed that the laser-induced fluorescence of fingertips is associated with blood, and so it is this signal that we used to determine blood volume (BV)[5]. However, *in vivo* experiments revealed a systematic decay of the BV measurement due to the laser itself. This effect was observed to be even stronger for diabetic patients[4]. Since blood volume is calculated by the integration of the fluorescence, this

observation indicates that, over a period of tens of seconds, there was a significant decrease in fluorescence produced by the exposed tissue. It is believed that this is a result of a light-induced chemical change, a process referred to as “photobleaching.”

Through further experimentation, it was discovered that static tissue, as opposed to blood, is the main photobleachable material. The purpose of this work is to identify, from the thousands of substances in static tissue, potential candidates which could be responsible for this “autofluorescence” (fluorescence by substances other than the one of interest, in this case, blood). We seek to observe their photobleaching properties that they may be appropriately accounted for to improve the accuracy of the blood volume reading and, concurrently, the blood glucose concentration determination.

Identifying a series of endogenous and exogenous substances is a difficult task. Given the nearly countless number of carbohydrates, proteins and smaller polypeptides, lipids, vitamins, antioxidants, and other biological molecules, it would require a massive effort to describe the photodynamic properties regarding the NIR and Raman spectroscopy of each of these substances to comprehensively isolate those which account for the autofluorescence and photobleaching events that have been observed. It is important to note that historically, due to technological limitations, spectroscopic investigations of such substances were performed using the ultraviolet-visible (UV-Vis) region of the spectrum, of

which there is already wealth of knowledge. However, since UV light in particular can damage and burn an exposed individual, UV-Vis spectroscopy cannot be utilized for *in vivo* experiments. Instead, near-infrared light is safe for vibrational Raman spectroscopy *in vivo,* and so is ideal for this technology. Due to the fact that there is far less literature pertaining to NIR spectroscopy than that of the UV-Vis range regarding specific substances of interest, the need for such investigation became apparent.

Therefore, based on structure and functionality, a series of vitamins, antioxidants, and the major skin pigment, melanin, were selected to ascertain their spectroscopic properties to identify potential fluorophores *in vivo* as well as to narrow down the list of skin-borne candidates. Antioxidants serve to protect essential cellular molecules from rapid oxidation by reactive oxygen species by themselves undergoing oxidation[6]. Since antioxidants contain loosely held electrons, which are essential to their function as reducing agents of reactive oxygen species, it was hypothesized that these molecules, as a class, might have excited electronic states low enough in energy such that long wavelengths, such as those in the NIR, could electronically excite them and cause subsequent fluorescence. Melanin has high absorptive properties, rendering it ideal as a skin pigment. With such high absorptivity, melanin became a candidate of interest as to its fluorescent and photobleaching properties[7]. Given its intricate macromolecular structure, which is yet to

be elucidated and under active investigation by other groups, melanin remains a compound which could provide great insight into the chemistry of photobleaching.

The literature demonstrates that advanced glycation end products (AGEs), namely pentosidine (the glycation product between ribose and the amino acids lysine and arginine), are highly fluorescent in the UV-visible[8]. The relatively high concentration of these ubiquitous substances in humans, the various biochemical pathways for their formation, and their association with diabetes patients who experience regular hyperglycemia attracted an interest into their NIR fluorescent and photobleaching properties. Since the present study began, we learned that pentosidine, AGEs in general, and hemoglobin do fluoresce and photobleach in the NIR. Since we now know at least three skin-borne substances that produce NIR fluorescence, this thesis is limited to all substances other than pentosidine and hemoglobin.

Literature Review

Raman spectroscopy theory

The theory of Raman spectroscopy derives from specific interactions between molecules and photons. When photons from nearly monochromatic light, such as from a laser, interact with matter, one of three events can occur. The light may pass through the molecule unaffected, it can be scattered, or it can be absorbed. Under *in* vivo

conditions, all molecules may exist in the ground electronic and vibrational states, which are of the lowest energy for a molecule. In the presence of light and other forms of excitation, the molecules can exist in various types of virtual states and vibrational states. During a molecule-photon scattering event, an incident photon of a given energy briefly distorts the electron distribution of a molecule, promoting the molecule from the ground state to a higher energy virtual state, and is then reflected in a different direction. If no energy is absorbed by the molecule, the molecule returns to its original energy level, and the photon is emitted at the same energy as prior to incidence, a process known as Raleigh or elastic scattering. If there is a transfer of energy between the light and the molecule, the photon is emitted at a different energy (and wavelength), leaving the molecule in a different vibrational state, a process known as Raman or inelastic scattering. The difference in energy between the incident and scattered light is equal to the energy of the vibrational transition[9,10].

Spontaneous Raman scattering is a fairly weak phenomenon, affecting only one in 10^6 to 10^8 photon/molecule interactions, and involves two types of processes: Stokes scattering and anti-Stokes scattering. Stokes scattering occurs when a molecule in the ground state absorbs some energy of the photon and is promoted to a higher energy vibrational state, while the photon emitted is of a lower energy and longer wavelength. Anti-Stokes scattering occurs when a molecule, already in an

excited state due to thermal energy, returns to the ground state and transfers energy to the photon, which is emitted at a higher energy and shorter wavelength. Stokes scattering is most commonly used for spectroscopic analysis; however, there are applications for anti-Stokes scattering. These shifts in wavelength are indicative of the structural features of the molecule, and therefore, the structures of compounds can be revealed by the investigation of their Raman spectra[9,10].

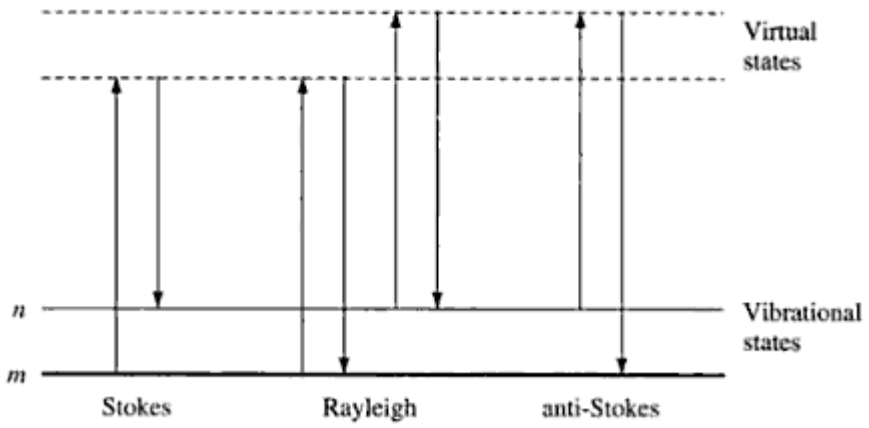

Figure 1: Graphical representation of Raleigh and Raman scattering processes. Source: *Modern Raman spectroscopy: a practical approach* by Ewen Smith, Geoffrey Dent[10].

Molecules may exist in different real quantum electronic states, either in the ground state or in more highly excited energy states. A molecule may be promoted from the ground state to the first excited state (or from one excited state to the next) if it absorbs an incident photon of an energy greater or equal to the energy difference between the electronic states. The excited molecule then will spontaneously relax from its excited electronic state to its ground state along with the emission of a photon through a process known as fluorescence. Beyond promotion to an

excited electronic quantum state, a molecule can be excited to higher energy vibrational states within the excited electronic energy level. Then, in a nonradiative process known as internal conversion, the molecule returns to a lower electronic state, but now containing substantial energy in the form of heat, i.e. vibrations[11].

As seen above, there are two distinct types of emission from such interactions: elastic and inelastic. The difference between them always pertains to the degree to which energy is transferred during the interaction[9]. Elastic emission results from no energy transfer, in which the reflected photon has the same wavelength and energy as the incident photon (Raleigh scattering). Inelastic emission involves energy transfer by inelastic scattering (Stokes and anti-Stokes) and fluorescence, in which the reflected photon has a different wavelength and energy from the incident photon.

Noninvasive in vivo Raman spectroscopy of human tissues

There is substantial evidence to link fluorescence with blood volume. Previous studies have shown that fluorescence fluctuates in coordination with cold-induced vasodilation, indicating an associated with blood volume[12]. Results of additional experiments on fluorescence changes and blood movement involving mechanical and thermal tissue modulation strongly imply the same conclusion[13]. Hemoglobin, the major oxygen-binding protein in blood, has been found be highly fluorescent in the NIR, and has also been proven to be a major component of blood

fluorescence[14]. For these reasons, the integration of overall fluorescence over time is used to monitor blood volume (BV). Through similar experiments, it has been found that elastic (Raleigh) scattering is strongly related to the volume fraction of red blood cells (RBCs). Likewise, the integration of the Raleigh line is used to monitor RBC volume; however, it has been observed that the elastic emission decreases as the RBC concentration increases, due to the dominant scattering coefficient in the tissues of the RBCs[15].

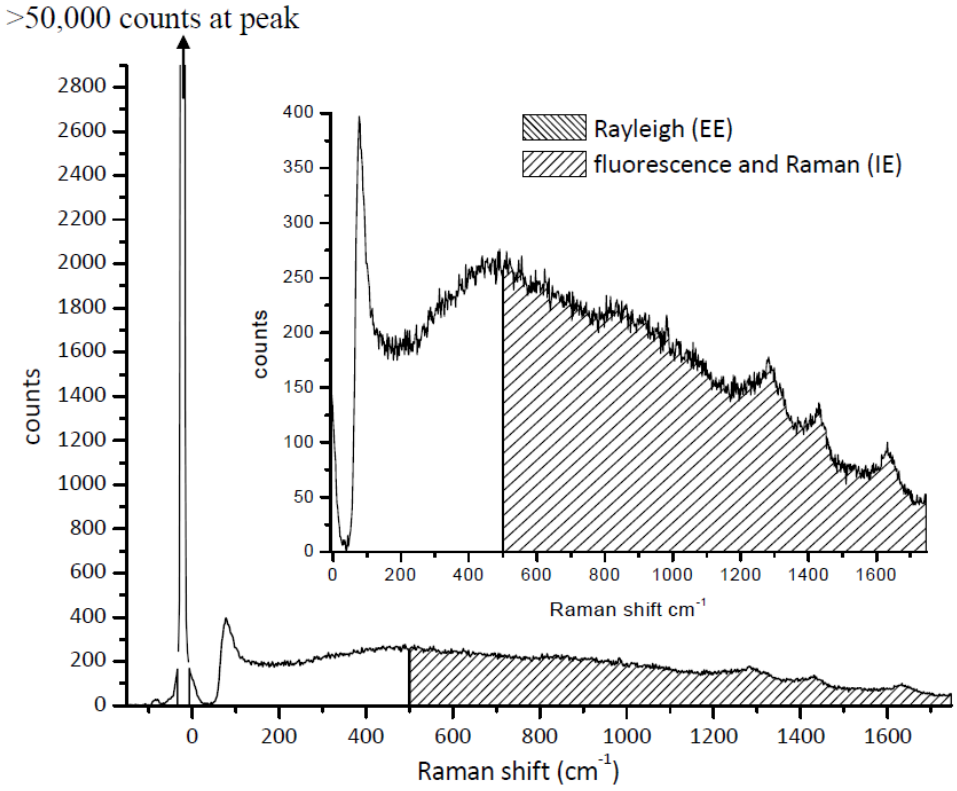

Figure 2: Intensity vs. frequency of a 20 ms CCD frame of a LighTouch® device using 830 nm excitation at 200 mW. Regions used to quantify inelastic scattering (500 cm^{-1} – 1750 cm^{-1}) and elastic scattering (-30 cm^{-1} – 10 cm^{-1}) are shown.

Displayed in Figure 2 is a typical emission spectrum of the volar side of a fingertip containing Raleigh, Raman, and fluorescence emission

during a 20 ms frame obtained using a LighTouch® device. The Raleigh line accounts for the elastic scattering that extends to above 50,000 counts. The sharp, variable Raman features due to inelastic scattering span the entire region of interest of the spectrum, and three particularly prevalent signals, the amide I, CH_2 deformation, and amide III, are visible at ≈ 1660 cm^{-1}, ≈ 1450 cm^{-1}, and ≈ 1270 cm^{-1}, respectively. Fluorescence is marked by the large broadband feature extending from ≈ 500 cm^{-1} -1750 cm^{-1}.

Fluorescence can be integrated and plotted as a function of time, the region of which is marked in Figure 2. Blood volume for a particular frame is calculated as the integration of the fluorescence band, which can be plotted as a single point on a BV vs. time curve. For a 200-second experiment, 10,000 such frames were recorded, yielding a graph such as that displayed in Figure 3. This curve represents tissue modulation used to obtain a spectrum of blood to determinate glucose concentration. During a mechanical tissue modulation event, there is an “unpressed” phase and a “pressed” phase. When tissue becomes pressed from a previously unpressed state, an external force presses against the dorsal side of the finger, modulating the skin of the volar side and forcing some interstitial fluids (i.e. blood) out of the region while static tissue and some fluids remain. If the difference between the spectra of the pressed and unpressed states is due to an efflux of blood as a result of applied pressure, the pressed phase can be subtracted from the unpressed phase

to yield a spectrum of blood (excluding static tissues). It is by this technique that blood glucose concentration is commonly determined[5].

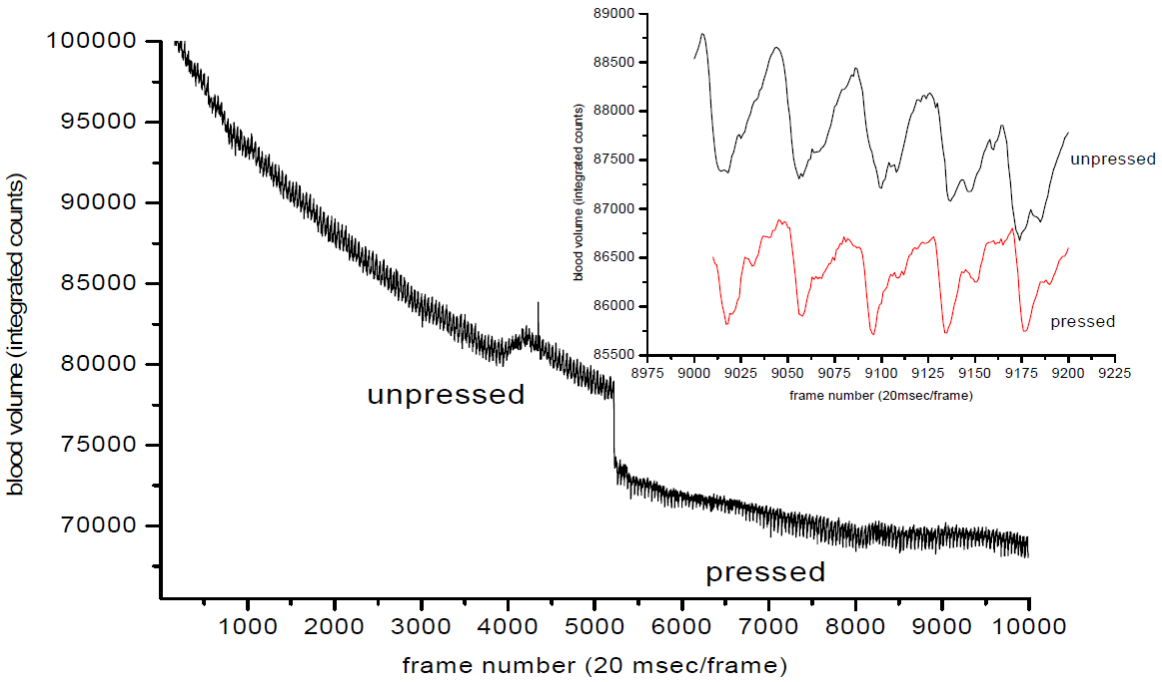

Figure 3: Typical BV vs. time curve of an experiment employing tissue modulation. The inset displays the same data between frames 2000-2200 to 9000-9200, from which pulses can be identified. A slight distortion due perhaps to movement of finger or additional pressure upon the aperture resulting in increased blood flow is noted at approximately 4200 cm^{-1}.

It is evident from Figure 3 that over time, excluding the transition between unpressed and pressed states, there is a significant decay through frame 4000 to approximately frame 8000, where it appears to level off. This decline has been evident in nearly every experiment that has taken place at LighTouch®. There is a significant change in fluorescence which is suspected to not be accompanied by a proportional change in blood volume. This regularly occurring phenomenon has recently been the target of inquiry, and the experimentation to identify the

cause of this decay is the purpose of the current study.

Problem of photobleaching

While it is certain that fluorescence is associated with blood volume, the relative contribution of blood to overall fluorescence is still yet to be determined. In fact, it is believed that most of the total fluorescence derives from substances other than blood, which are present in the surrounding static tissues. In order to see how one might approach this question quantitatively, we note that in these types of experiments, light penetrates the finger hundreds of microns below the surface of the skin, and engages in interactions within a defined volume of tissue. Of this defined volume of the volar side of a fingertip prior to systole, 97% is composed of static tissue, and 3% is composed of blood residing in blood vessels such as capillaries. It has also been reported that within these vessels, the hematocrit (the volume fraction of blood occupied by red blood cells) is approximately 0.10, so in the resting state, 2.7% of the total volume is composed of plasma, while 0.3% is composed of red blood cells. Therefore, given that each component has a different fluorescence per unit volume, the contribution of each component to the total fluorescence can be described by the following equation, where *a, b,* and *c* are the fluorescence per unit volume coefficients of static tissue, plasma, and red blood cells, respectively:

$$0.97(a) + 0.27(b) + 0.03(c) = \text{Total Fluorescence} = BV_{(diastole)}.$$

During a pulse, there is an influx of blood in the blood vessels, and,

assuming there are no voids, this additional blood volume displaces the same amount of static tissue volume from the irradiated region. Also, assuming that the hematocrit remains constant, the peak of systole, during which blood volume is doubled and the static tissue volume decreased by the same amount, can be described by the following equation:

$$0.94(a) + 0.54(b) + 0.06(c) = \text{Total Fluorescence} = BV_{(systole)}.$$

While the precise amount of increase in blood volume during a pulse is uncertain, this situation, with its assumptions, provides a useful model to account for the contribution of the different components to the observed fluorescence over time. Since we routinely collect 10^3–10^4 BV vs. time measurements and an equal number of RBC vs. time measurements, we have a large, overdetermined system of two equations, two unknowns, which can be used to obtain relative tissue volume fractions in the NIR-probed volume. The model indicates that when the volume fraction of one component increases, that of at least one other must decrease, because the sum of all volume fractions must equal unity, so long as there are no voids.

However, one of the most important assumptions about blood volume and fluorescence is challenged by the phenomenon of photobleaching. If it is assumed that the fluorescence per unit volume for each component remains constant, then changes in fluorescence can be only caused by the movement of these components, namely blood. The fact that during experiments there is regularly a decay of 15-20% in

fluorescence can be explained only by one of two possibilities. If the assumption is true, the decline in fluorescence results from a substantial efflux of fluorescent material out of the irradiated zone. Studies of hydrostatic blood movement due to gravity decreases make such blood movement seem unlikely[20]. The more plausible explanation is that there is a chemical change in one of the components, most likely in the static tissue, where certain substances are transformed into less fluorescent products (i.e. they are photobleached). Therefore, the phenomenon of photobleaching poses a significant obstacle to accurately determining blood glucose concentration. Further understanding of the substances that undergo this process and the products that are formed is essential to improving upon *in vivo* noninvasive analysis by Raman spectroscopy[4].

Pentosidine

High levels of pentosidine in diabetics can be explained by the fact that pentoses can be formed from hexoses by means of a series of metabolic reactions known as the pentose phosphate pathway (also called the hexose monophosphate shunt). Glucose-6-phosphate undergoes a dehydrogenation step to form a lactone, followed by hydrolysis, and then oxidative decarboxylation to form ribulose-5-phosphate, while two equivalents of NADP+ are reduced to NADPH and carbon dioxide released to drive the reaction forward. Ribulose-5-phosphate and other pentose phosphates such as ribose-5-phosphate and xylulose-5-phosphate can be interconverted by action of isomerase and epimerase

enzymes[16].

It is this pentose pool, of which its biological intention is to synthesize macromolecules that incorporate pentoses such as RNA and DNA or to continue through the non-oxidative stage of pentose phosphate pathway to form glycolytic intermediates, which provides the basis for the formation of the highly fluorescent pentosidine[16]. Formed by Maillard chemistry, pentosidine is used to indicate the relative presence of advanced glycation end products (AGEs) which can result from oxidative stress and, notably, hyperglycemia by means of the described pentose phosphate pathway[17]. If an individual has a high level of glucose leading to high levels of pentose and therefore pentosidine, it can be suggested that this mechanism explains why the tissue of diabetics seems to fluoresce much more than those who have not experienced regular long-term hyperglycemia. Due to the fact that its potential as a photobleachable material was only realized after these experiments were performed, the study of pentosidine is not included in this text. However, the investigation as to the chemistry underlying the photobleaching of pentosidine is currently taking place.

In vivo investigation

Experimental

In vivo Raman instrument

While a complete description of the instrument known as a LighTouch® device, used for *in vivo* experiments, is beyond the scope of

this thesis, a diagram of the system utilizing Raman spectroscopy to obtain information from human tissue, such as blood glucose concentration and hematocrit, is displayed in Figure 4. A CW external cavity diode laser is used to produce a 45 mW excitation of 805 nm, though other lasers can be substituted to perform experiments using 785 nm or 830 nm light. The light passes through a Semrock clean-up filter and then through a focusing lens, so that the light focuses precisely at the aperture, at which a fingertip is placed[4]. The 2 mm aperture is in a spring steel plate providing the surface against which an individual presses his finger. The laser spot at the finger is approximately 100 x 230 μm, and is elliptical in shape. The angle of incidence of the light to the finger is about 53°. The emission is collimated as it passes through a pair of lenses to reorient the light parallel and through a “Razor Edge” filter to reduce the signal due to Raleigh scattering, and is then refocused onto a 60 fiber x 100μm bundle of fused silica fibers[14]. The fibers introduce a line image to the Process Instruments f/2.1 spectrograph that is detected by a Critical Link CCD camera, cooled to -80 ℃. Not shown are two electronic shutters between the clean-up filter and the coupling lens that allow for pulse sequences of the laser to the fingertip. The entire optical apparatus is enclosed within a black casing to prevent outside light from entering the system[4].

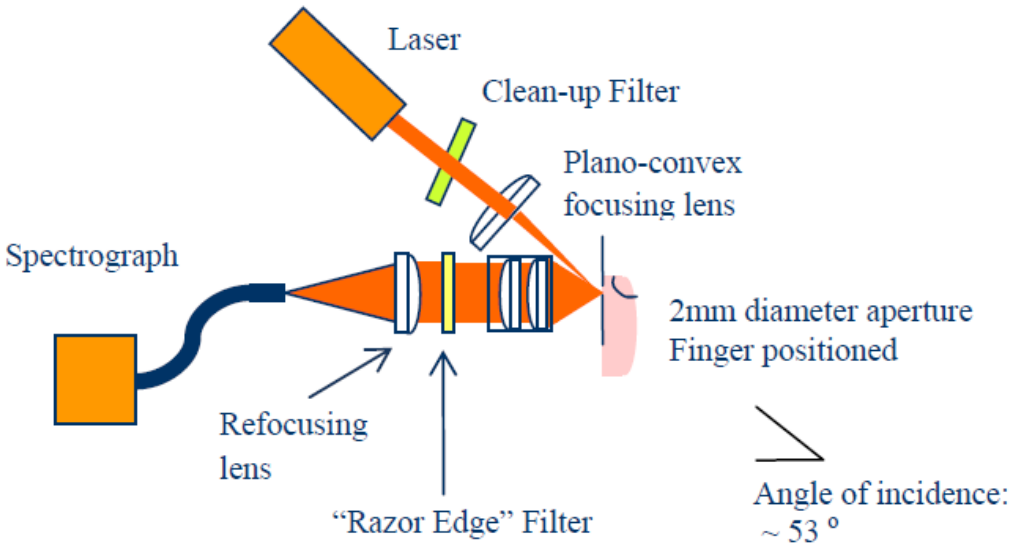

Figure 4: Schematic diagram of *in vivo* LighTouch® device optical layout.

A variety of "human error" can influence the data. Pushing one's finger against the aperture can cause the tissue to excessively extrude through the hole, an effect called "doming", changing the path length of the laser through the tissue, which alters the scattering processes necessary for an accurate measurement. Moving one's finger during the measurement process can change the types and amounts of tissues interacting with the light and producing emission. In order to establish a protocol that can be replicated by non-experts to reliably reproduce data and minimize errors, a force measurement and placement system has been added to the apparatus containing the aperture to control pressure and position[18].

The position detector-pressure monitor (PDPM) involves a series of small gold-plated dots built into a circuit board, above, below, and to the left and right of the hole. The resistance is lower when tissue is in contact

with the gold dot than when there is no contact. If a finger is or is not in contact with a gold dot, the appropriate electronic signal is transmitted by the circuit board to the computer. Therefore, position and contact area can be monitored at all times prior to and during the experiment. A force transducer, coupled with a lever system, is used to detect the force applied by one's fingertip at the aperture. Force and pressure can, therefore, also be monitored throughout the experiment. These features are coordinated with a graphical user interface (GUI) which allows individuals to easily center their finger on the aperture and to recognize if they are pushing too hard against the aperture[18].

An automated force actuator is used to achieve tissue modulation. This servo-driven device applies a uniform pressure by applying force according to the contact area detected by the PDPM. This pressure causes skin and underlying tissues to extrude through the aperture, and also causes some movement of fluids, such as blood, out of the irradiated area[18]. The pressure can be adjusted by the experimenter, and to collect data using tissue modulation involving a "pressed" state and an "unpressed" state, an experiment is set up such that, during the first half, a relatively low pressure is applied, and is then raised during the second half. Pulse modulation is another technique used to obtain a spectrum of blood that does not utilize differences in pressure[19]. For the purposes of studying fluorescence and the photobleaching of static tissues, neither technique was applied. However, the force actuator was necessary to

maintain consistency in all experiments.

For a typical experiment, the test subjects were asked to insert their right-hand middle finger into the apparatus and, using the GUI as a guide displaying the gold dots on the circuit board, center it over the aperture. During the set-up phase, the test subjects press gently on the aperture and are given time to ensure both that the finger is properly placed and that they are comfortable enough to remain in position for the duration of the experiment. The subjects are asked to remain passive while the actuator is brought in contact with the dorsal side of the finger and brings the finger to ≈ 15 g/cm^2 pressure against the aperture. Once the collection is started, the actuator increases the pressure to, for example, ≈ 60 g/cm^2, and the shutters open to allow exposure of the finger to the laser. The pressure is held constant for each experiment and is designed to be approximately halfway between diastole and systole. This device can do this with much greater accuracy and measure than the human hand[18].

In vivo experiment protocol

Two major experiments were performed to establish the contribution of blood and static tissue to the commonly observed decay in fluorescence. The first was aimed at determining the effect of inducing hydrostatic relaxation. Hydrostatics is an integral part of understanding the circulatory system and is complicated by a number of factors. Hydrostatic pressure is the force exerted by a fluid as a result of gravity, and it has been found that the hydrostatic pressure in blood can be affected by body

position as well as muscle contraction. The process of performing exercises involving these factors to achieve a state of equilibrium is known as hydrostatic relaxation[20]. For each of three different trials, data were collected following a protocol associated with the LighTouch® device, and the integrals of the elastic emission and the inelastic emission were recorded over time. Since RBC volume is associated with elastic emission, and blood volume with fluorescence, the integrals of the EE and IE of frames recorded by the CCD as a function of time are used to monitor RBCs and BV, respectively.

Each test subject was first asked to equilibrate the blood in his or her hand (flexion of muscles as well as stretching and overall body movement) and then insert a middle finger into the apparatus for set up, while a pressure of ≈ 15 g/cm^2 was applied. The pressure was increased to ≈ 60 g/cm^2, and a 100 second measurement (A) was then recorded with laser exposure. Immediately after, the finger was left motionless while the pressure was reduced to ≈ 15 g/cm^2 for about 10 seconds. The pressure was again raised to ≈ 60 g/cm^2 and another 100-second measurement (B) was recorded without cessation of laser exposure. Upon completion, each subject was asked to re-equilibrate his or her arm and hand and the finger was inserted at a slightly different position. The pressure was applied and then raised while the finger was left motionless, as if for the previous measurement, except that no laser exposure occurred during this period. Then, as in B, the finger was set up with the appropriate pressure

changes, laser exposure was resumed, and another 100-second measurement (C) was recorded.

The second experiment focused on the effect of the laser on fluorescence recovery. First, the fingertip was set up in registration with the aperture, and the pressure was brought to ≈ 60 g/cm^2 with the laser blocked, marking t=0 s. At t=2 seconds the laser was unblocked, exposing the finger. The measurement was allowed to continue, and at t=27 s, the laser was once again blocked for 8 seconds, until t=35 s, to allow over a dozen cardiac pulses to displace the previously exposed blood with unexposed blood in the irradiated volume. At this point, the laser was again unblocked, and the experiment was allowed to proceed until t= 41 s, when again the laser was blocked and remained so until the end of the 50-second period. The BV vs. time plot from the collected CCD frames was then analyzed.

Results

Figure 5 shows the RBC vs. time and BV vs. time plots acquired from the hydrostatic relaxation experiment. The BV curve of A exhibits the decay in fluorescence, with a sharp drop off in the first 3 seconds, a continuing steep decline through 20 seconds, and a steady decline until t=80 seconds, when it appears to have leveled off at just about 80,000 integrated counts. The BV curve for B, a result of the trial about 10 seconds after A to allow fresh blood to circulate into the region, does not undergo the decline that is evident for A; there is a steep drop off in the

first 2 seconds, but the fluorescence appears to be stable between 76,000-78,000 counts throughout the duration of the measurement. It is noted that the fluorescence recorded throughout B is approximately the same as that which was observed at the end of A, when it seemed to stabilize after undergoing the decay. Also, the RBC curves representing the integrated elastic emission for A and B appear nearly identical and remain stable throughout the course of each measurement. The BV data of measurement C following hydrostatic relaxation reveals a pattern similar to that observed for A.

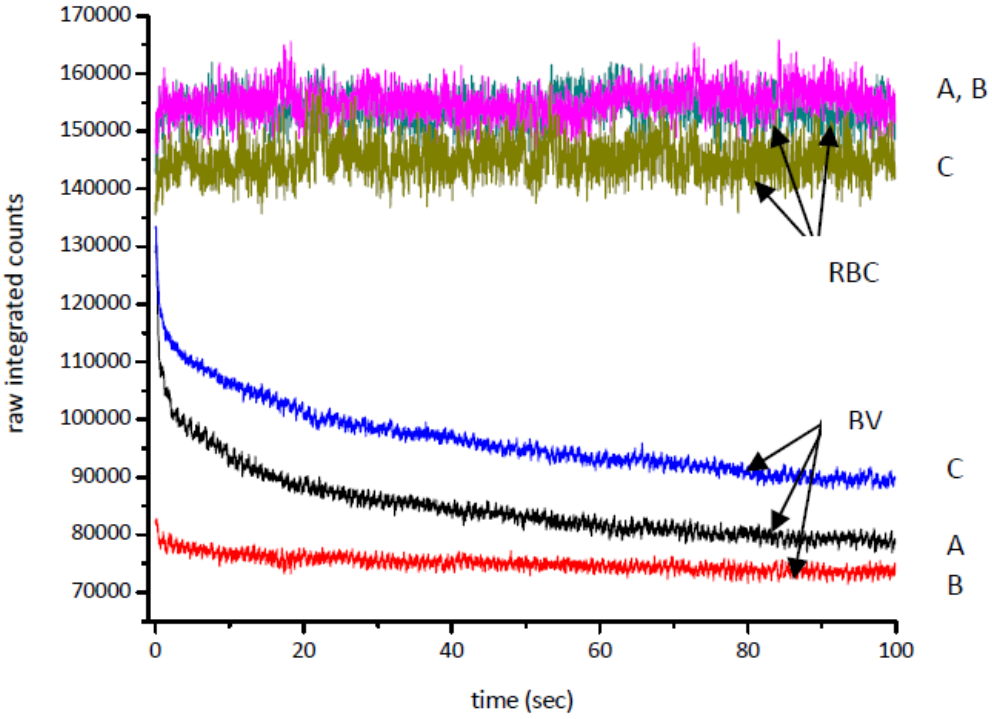

Figure 5: BV vs. time and RBC vs. time curves of the hydrostatic relaxation experiment. Condition A) initial 100 s with exposure and hydrostatic relaxation; condition B) second 100 s with exposure and hydrostatic relaxation after remaining motionless 10 s after A; condition C) 100 s with exposure remaining motionless following 100 s with hydrostatic relaxation, but not exposure.

Fluorescence decayed in a homologous fashion and then seemed to

reach a stable level at t=80 s. It was observed, however, that overall fluorescence and decay in trial C was greater than in A, and that the RBC count was lower than in trials A and B. It was shown that the changes in fluorescence were not a result of blood movement.

The results of the experiment focusing on the effect of the laser on fluorescence recovery are displayed in Figure 6. The integrated fluorescence BV curve shown represents data obtained using the typical isobaric experimental procedure, and the only variable modified at different points in the experiment was whether or not the laser was blocked, allowing or preventing exposure. It is obvious that, because the experiment began with the laser blocked, fluorescence was at zero until it spikes at t=2 s, when the laser was unblocked. From this point until t=27 s, the fluorescence decays in the manner that has been previously described. There is a sharp decrease in the first 7 s of exposure, and then the decay becomes slightly more moderate from t=10 s to t=20 s, at which point it appears to level off until t=27 s. Note that the apparent fluorescence never falls completely to zero because of the dark current detected by the CCD camera, regardless of whether or not the laser is blocked.

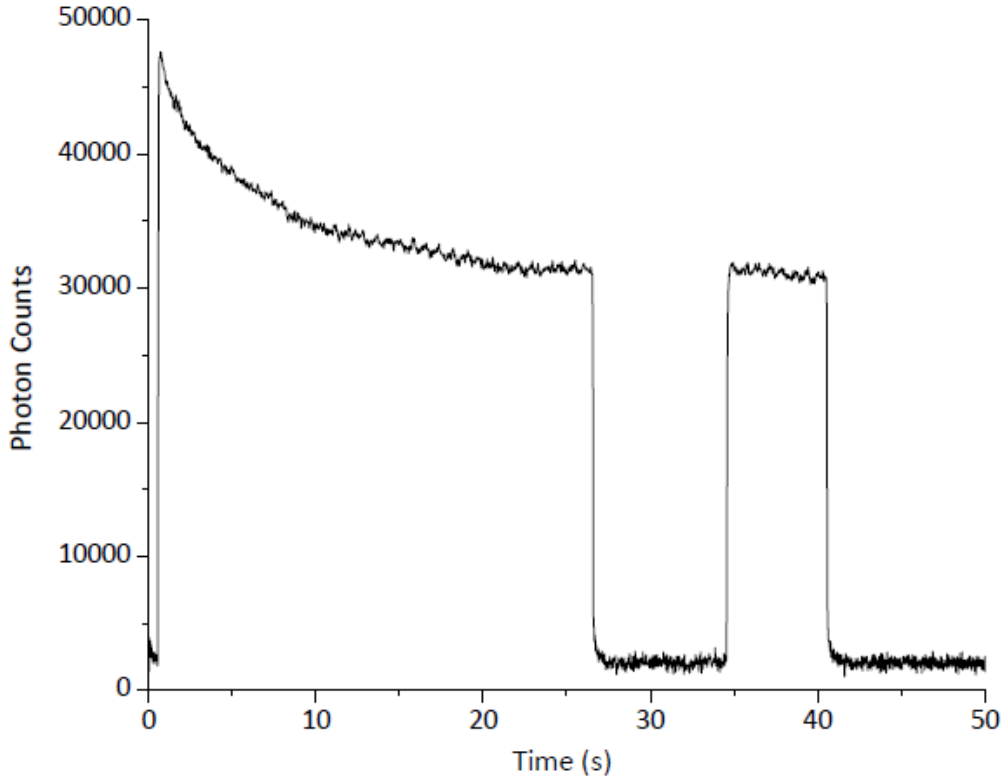

Figure 6: Integrated fluorescence BV vs. time curve from the study to observe fluorescence recovery. Laser exposure of finger was allowed by unblocking the laser from t=2 s to t=27 s and from t=35 s to t=41 s. The fluorescence decayed 33.7% over the course of the experiment.

At this point, when the laser was blocked, the fluorescence dropped to its minimum and remained so until the laser was unblocked at t=35 s, permitting exposure to the finger. At this time, the fluorescence recovered to a point nearly identical to that immediately before t=27 s when the laser was turned off; no significant increase was observed. The fluorescence then decayed in a rather slow fashion until t=41 s, when the laser was again blocked until the end of the 50 s period. Because the initial fluorescence at t=2 s is roughly 47,500 counts and the fluorescence seems to equilibrate at around 31,500 counts, the overall decay in fluorescence is 33.7% of the original value.

In vitro investigation

Experimental

In vitro Raman instrument

The device used to collect Raman spectra of samples *in vitro* (schematic shown in Figure 7) employs a gallium arsenide external cavity diode laser to produce an excitation of 785 nm at 450 mV. The laser *primarily* produces a wavelength of 785 nm, but because the Raman signal is so weak, a filter is used to ensure that no additional light even near 785 nm reaches the detector[4]. The light then passes through a lens used to narrow the diameter of the laser spot to 200 µm, and is reflected by a mirror angled at 45º to normal. After passing through a small hole in the mirror, the light reaches the sample at normal incidence. Solid and liquid samples can both be accommodated using the apparatus. Solid samples such as powders were placed in wells within the plate, which were then placed under the laser, whereas liquid samples were placed in a 2 mL glass cuvette, which was then positioned under the laser by use of a customized holder. Occasionally, small bubbles arose to the top of the cuvette, and in this event, the cuvette was tapped to let the bubbles escape, to ensure that the spectrum was not affected.

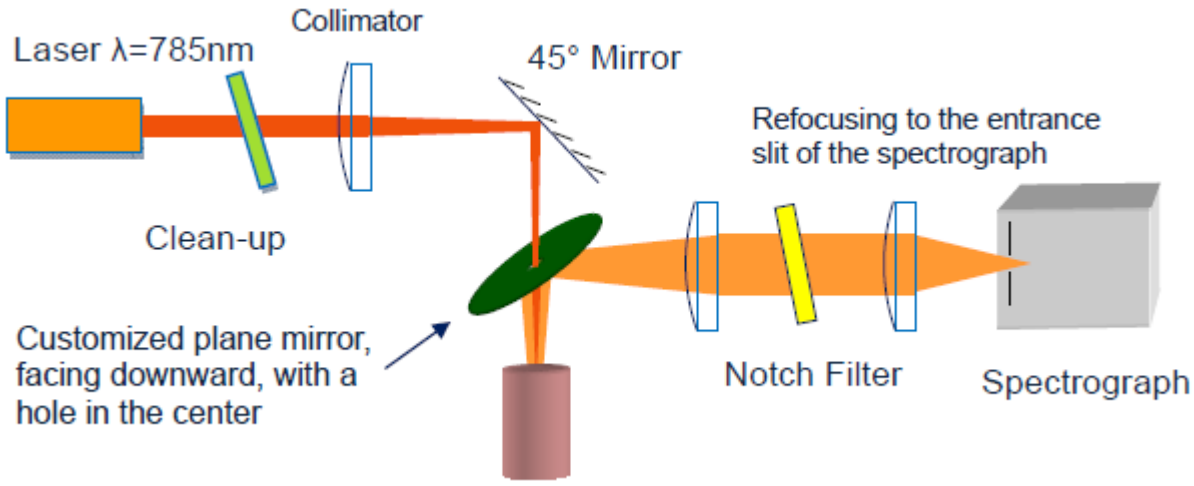

Figure 7: Schematic diagram of *in vitro* Raman spectroscopy device optical layout.

Any light from scattering or fluorescence emitted upward is reflected by a mirror facing downward in the direction of the spectrograph. A focusing lens is used to reorient the direction of the broad emission, such that the light beams parallel. The light then passes through a notch filter, which blocks the higher energy component of the signal including the Raleigh line, so that it does not affect the Raman features[4]. A refocusing lens then narrows the broad parallel signal into a small spot, so it can pass through a small slit to reach the Kaiser f/1.4 Holospec spectrograph. The spectrograph disperses the light to the Roper Scientific/PAR CCD camera, where it is quantified and converted into a data form that is sent to a computer for processing[21]. The CCD camera is cooled using liquid nitrogen to maintain a temperature of -196 ºC to improve the signal-to-noise ratio.

WinSpec32 is the software used to operate the Raman device, set up experiments, and visualize the raw spectra that are produced. Various

aspects of each experiment can be controlled, including the number of spectra collected, the number of exposures, and the length of exposure. Typically, longer experiments yield a higher signal-to-noise ratio[18]. While generally it would be ideal to perform long experiments on all samples, because some substances have been observed to photobleach and recover, in many experiments several successive spectra, each obtained over a short period of time, were collected. The changes in fluorescence between short intervals can be observed over a long period of time as a result of exposure, rather than collecting one spectrum providing information regarding the length of time as a whole, revealing nothing about incremental changes. Further data analysis was performing using the software OriginPro 8.

In vitro experiment protocol

Experiments were performed to ascertain the spectroscopic properties of L-glutathione, uric acid, β-carotene (the precursor to vitamin A), cholecalciferol (a form of vitamin D), L-ascorbic acid (vitamin C), and ±-α-tocopherol (a form of vitamin E). To understand the contribution of these substances to the emission from human tissue resulting from NIR exposure, these experiments were designed to simulate physiological conditions by studying the Raman and fluorescence features of these compounds at different concentrations, relative to their respective normal concentrations in blood, interstitial fluid, or skin.

Different concentrations of each sample were made by creating a

stock solution, either saturated or of a high enough concentration that the solution itself could be accurately made, followed by a series of dilutions. It was important to obtain spectra at different concentrations, because not only is it essential to determine whether or not a sample fluoresces, but also, if a particular substance does fluoresce, to establish a means to quantify its contribution to the overall fluorescence. Moreover, many other variables (such as turbidity) must be taken into account, which are best identified by obtaining spectra of compounds at different concentrations. The cuvette in which the solutions are held also fluoresces, and there are often losses of emission due to self-absorption, as well as scattering, which can lead to ambiguous spectroscopic observations.

While an attempt was made to include data on all compounds at their physiological concentration, it was believed that some concentrations were too low to be detected by the CCD, so greater concentrations were used. At each concentration for each compound, ten-minute experiments to produce a single spectrum were performed. From the spectra, the features of different substances were compared, along with differences due to concentration of a single compound. The concentrations of the antioxidants and vitamins used are displayed in Table 1.

Table 1: Experimental concentrations and physiological concentrations (in blood, interstitial fluid, or skin) of antioxidants studied.

Name	Solvent	Physiological Concentration[22]	Experimental Concentrations (mM)
L-Ascorbic Acid	Deionized water	50-60 µM	187.5, 7.5, 0.3, 0.06
Reduced Glutathione	Deionized water	≈1.09 mM	81.25, 3.25, 0.65
Uric Acid	Deionized water*	234-456 µM	Saturated, 0.8, 0.4
Cholecalciferol	Cyclohexane	40-80 nM	6.25, 0.25, 1.0×10^{-2}, 4×10^{-4}, 8×10^{-5}
β-carotene	Cyclohexane	1.23-1.75 µM	3.13, 1.56, 0.78, 0.13
±-α-tocopherol	Cyclohexane	≈24 µM	1.25, 0.16, 0.05

Due to solubility difficulties encountered, only a close approximation of the concentrations of β-carotene solutions were made. A saturated solution of uric acid of unknown concentration was analyzed. *Uric acid was dissolved in NaOH in deionized water solution at pH≈ 8.

Solubility was a recurring obstacle throughout these experiments. Vitamins are generally divided into two categories: water-soluble and fat-soluble. Therefore, as expected, only two substances analyzed (ascorbic acid and reduced glutathione) were soluble in deionized water at room temperature. The organic solvent cyclohexane (ACS spectrophotometric grade, ≥99%, Sigma-Aldrich) was chosen for the experiments for the fat-soluble vitamins. While ±-α-tocopherol and cholecalciferol did successfully dissolve in cyclohexane, β-carotene and uric acid presented solubility issues. Therefore, saturated solutions of these compounds were prepared (β-carotene in cyclohexane and uric acid in NaOH in water solution pH≈8), of which the concentrations could only be estimated, as some solid particles were still visible. A saturated solution of β-carotene was decanted from the insoluble particles, and dilutions were then subsequently

performed. For uric acid, a saturated solution was first prepared in addition to 0.8 mM and 0.4 mM solutions.

Similar experiments were performed with the pigment melanin, which presented an even more complex solubility dilemma. Melanin is reported to be slightly soluble in water, but this varies due to its complex structure[4]. Therefore, various dissolution and filtration steps were taken. Synthesized eumelanin, a dark brown powder (Sigma-Aldrich), was added to water to form a very dark, opaque, grey-brown solution, with solid particles resting at the bottom of the beaker; these were broken into smaller particles using a glass rod. Using a 100 nm Whatman syringe-filter, the solution was filtered to yield a clear solution. However, after this mixture was allowed to rest in the refrigerator for four months, a great deal of what appeared to be solid insoluble melanin had settled to the bottom of the beaker, while a clear yellow solution remained as the supernatant. This supernatant was extracted from the insoluble particles. When this solution was filtered, some of the color was lost, but the solution retained its yellow tint. It was believed that, over time, some of the melanin had broken down into smaller, soluble units that would not present any loss of signal due to elastic scattering, i.e. turbidity (the cloudiness caused by large insoluble particles). This final melanin solution, labeled the “stock” solution, was then diluted to various concentrations (10%, 20%, 50%, 60%, and 80% of stock solution) and each solution was then analyzed. Because of the initial filtration of melanin, neither the molar concentration nor the concentration

by mass could be estimated. For each concentration sample, thirty-minute measurements were performed to obtain Raman spectra.

By studying the spectra of various substances *in vitro*, several key determinants of interest were measured. Whether or not a substance fluoresces as a result of NIR excitation was identified by a spectrally broad emission apparent on its spectrum. Should the species not fluoresce, it is important to note that, while they may have distinctive Raman features, these substances likely do not contribute to fluorescence and photobleaching in human fingertips. Based on the fluorescence results, melanin was the only substance which was studied in terms of the dependence of fluorescence on concentration, as well as on the processes of photobleaching and recovery.

The dependence of fluorescence on the concentration of melanin was determined by plotting the integral of the fluorescence as a function of concentration. This can be useful for quantifying the contribution of a particular substance to the total fluorescence *in vivo*. The integrated fluorescence of the four different concentrations of melanin was plotted

The next goal was to determine whether or not melanin photobleached, and if it did, to gain an idea of the kinetics of the process. If a substance photobleaches, the total fluorescence of the sample decreases over time as a result of prolonged laser exposure. Using the filtered saturated solution of melanin, over the course of an hour, thirty two-minute spectra were collected. The integral of the fluorescence of

each measurement was then included as a single point on an integrated fluorescence vs. time plot, and any decay in fluorescence was apparent.

Finally, once melanin was found to fluoresce and photobleach, the next task was to find if the substance recovers its fluorescent properties following photobleaching. This was ascertained by first performing an experiment identical to the one previously described above to monitor the photobleaching of a substance over a period of time. Then, while leaving the sample in place and keeping the room lights off, the laser was blocked, and the sample was left in the dark for varying amounts of time, two hours or twelve hours. The experiment of collecting thirty two-minute spectra over short intervals was then repeated. By comparing the two experiments, it was apparent if the substance had recovered after it had been photobleached, and by how much after a given length of time.

It is important to note that any solvent, including water and cyclohexane, can produce emission[10]. The spectra of pure cyclohexane and deionized water are displayed in Figure 8. While water has a fairly weak emission (allowing Raman spectroscopy to be ideal for *in vivo* studies) the signal for cyclohexane is quite strong, the baseline being over double the overall signal of water, with several strong features, due to C–C and C–H vibrational modes[9]. There is also signal that is detected by the camera even there is no laser excitation, known as dark current, which affects the spectra in a similar way, though dark current was not subtracted from the spectra in Figure 8. Water, cyclohexane, and the

cuvette all have not been observed to photobleach.

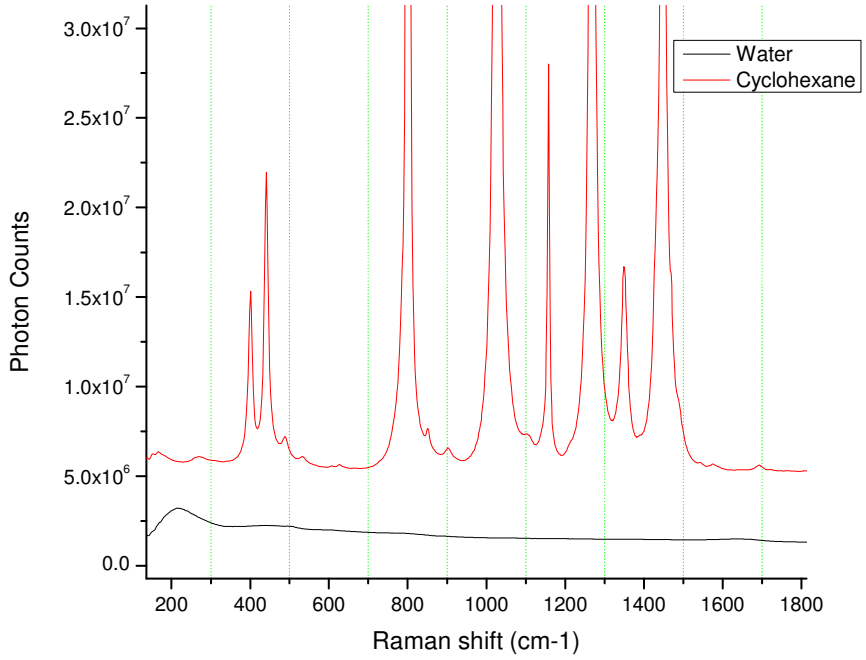

Figure 8: Emission spectra of pure cyclohexane and deionized water.

Due to the fact that each of the species of interest are present in relatively low concentrations, the emission due to water can cause the data to be misleading, since prominent features can be the result of the solvent instead of the solutes, which can also mask their key features. For this reason, when possible, the raw data are paired with those from which the corresponding solvent spectrum has been subtracted, a technique called “baseline subtraction”, so that signal due to the solute can be isolated and characterized. However, when a clean subtraction was not possible (commonly encountered with cyclohexane as the solvent) only the raw data are shown.

Results

Antioxidants

The emission spectra of L-ascorbic acid depicted in Figure 9 show a pattern that was often observed during these experiments. From the raw spectrum, it appears that each emission follows the general trend set by the background combined emission of the cuvette and water solvent, involving a greater signal sloping downwards from 300 to 1000 cm^{-1}, with broad gentle peaks at 430, 605, 790 and 1640 cm^{-1}. However, it is clear, most evidently from the baseline subtracted spectra, that L-ascorbic acid produces emission in addition to that of water. The L-ascorbic acid spectrum at a concentration of 187.50 mM displays many sharp vibrational modes of the molecule, but no fluorescence. However, if the concentration is decreased by a factor of 25 or more, most of these features all but disappear. While they do all produce a steady emission that is greater than water, it appears that solutions of the three lower concentrations do not exhibit strong Raman features. Given that overall emission from the data increases in the order, by sample, of 0.06 mM, 7.50 mM, and 0.03 mM, it is believed that L-ascorbic acid does not produce significant signal at such low concentrations, and any differences in the spectra could be a result of differences in the placement of the cuvette. It is concluded that, at its physiological concentration, L-ascorbic acid is not a significant contributor to the fluorescence of human tissue.

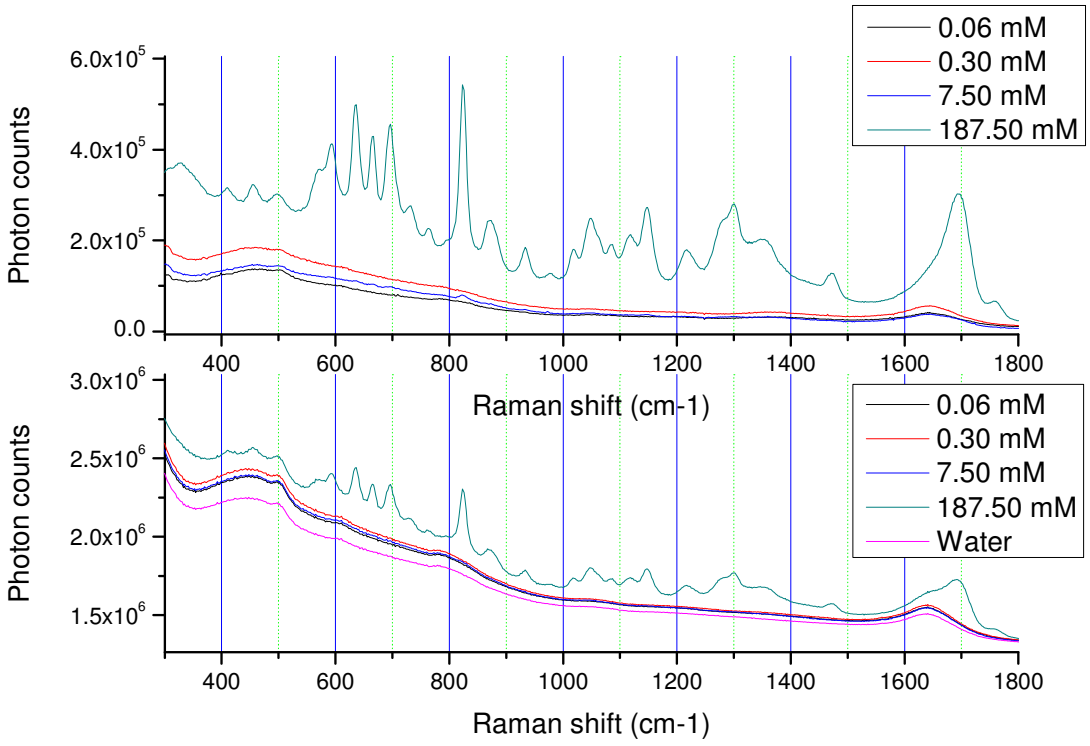

Figure 9: Subtracted (top) and raw non-subtracted (bottom) spectra of L-ascorbic acid at varying concentrations from 300-1800 cm^{-1}. It is noted that while the spectra at the highest concentration exhibit many noticeable vibrational features, at concentrations of 7.50 mM and less, most are hardly distinguishable.

It has been previously documented that β-carotene has a strong resonance Raman spectrum, and is also known to be highly absorptive in the visible spectrum, hence its function as a pigment[23]. However, it appears, from these experiments performed, that β-carotene does not fluoresce as a result of NIR excitation. The spectra displayed in Figure 10 reveal that β-carotene produces very strong Raman emission centered at 1010, 1155, and 1520 cm^{-1}, smaller peaks at 950 and 1180 cm^{-1}, and weak emission underlying from 800 to 1620 cm^{-1}. As shown in Appendix A, the integral of the peak centered at 1520 cm^{-1} was plotted as a function of

concentration, and it was found that there does appear to be a linear dependence (slope = 1.234×10^{8}, $R^2 = 0.935$, and standard error = 1.853×10^{7}). This pattern holds true for the additional Raman signals. While it is shown that the Raman emission of the substance increases linearly with concentration, it is apparent that β-carotene does not fluoresce as a result of NIR excitation, and therefore must also not be a contributor to human tissue fluorescence.

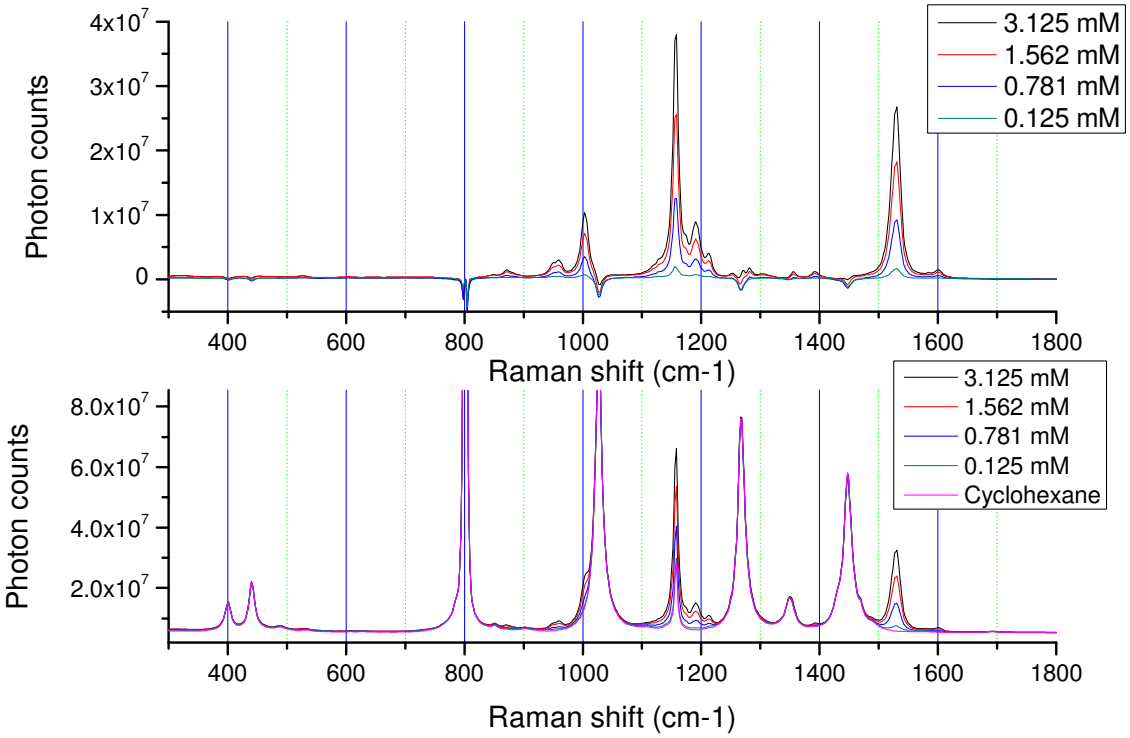

Figure 10: Subtracted (top) and raw non-subtracted (bottom) spectra of β-carotene in cyclohexane at varying concentrations. The peak at 1040 cm^{-1} extends to nearly 1×10^{8} counts, while the peak at 800 cm^{-1} extends to nearly 1.6×10^{8} counts.

The remaining spectra of antioxidants are included in the appendices. Reduced glutathione (spectra shown in Appendix B) follows a

trend similar to that of L-ascorbic acid, but to a lesser extent. Most of the Raman emission from the glutathione solutions follows the water baseline, but it is apparent that there is additional emission due to the solute. There appears to be no fluorescence emission. At the highest concentration (81.25 mM), there is a steady Raman emission throughout the 300-1500 cm^{-1} range, with several peaks. The spectra of the two lowest concentration solutions show very little difference both from water and from each other. However, it can be noted on the subtracted spectrum of the 3.25 mM solution that there are some peaks (500, 610, 800, 1040, and 1430 cm^{-1}) corresponding to those on the spectrum of the 81.25 mM solution; these have been significantly broadened as a result of the low concentration. As expected, it appears that the signal increases as the glutathione concentration increases, but the signal is so weak at physiological concentration that it is nearly impossible to distinguish it from water. Glutathione, despite being at the highest physiological concentration of all the antioxidants studied, is also not a likely contributor to tissue fluorescence.

Uric acid produces only minimal emission in addition to the background signal and does not seem to fluoresce, but the spectra produced (displayed in Appendix C) present a somewhat interesting pattern. The overall signal appears to decrease rather than increase as the concentration of uric acid increases. This phenomenon indicates that there must have been a signal loss whose effect strengthened as the

concentration of uric acid particles increased. While loss of signal is often a result of absorption, it appears that this scattering loss may have been caused by the turbidity of the solution.

Turbidity involves the suspension of undissolved particles, and because uric acid is relatively insoluble in water, which was somewhat resolved by increasing the pH of the solution, it is possible that the uric acid solid did not fully dissolve. These relatively large particles scatter light more effectively than the small dissolved particles, and resulting in a decrease in emitted light. Because there were likely more of these large particles at the higher concentrations, because the solution was not filtered, it is believed that the increased turbidity at high concentrations reduced the signal. Different placements of the cuvette may have also affected the spectra of uric acid at low concentrations. Nonetheless, the signal at physiological concentration is so weak that it is not likely that uric acid contributes to NIR tissue fluorescence.

Just as for uric acid, it was observed from the spectra of ±-α-tocopherol (a viscous yellow oil), which is displayed in Appendix D, that the overall signal increased as the concentration decreased. While it is possible that turbidity and a loss by scattering could have affected the signal, this is believed to be unlikely, because ±-α-tocopherol did not seem to present any solubility difficulties. The trend may have been the result of a loss by absorption; or, because the difference appears to be so minute, a difference in the placement of the cuvette, which also fluoresces

significantly, could have affected the spectra. There appears to be very little Raman signal beyond the cyclohexane emission, and there is no apparent fluorescence.

The spectra of cholecalciferol, displayed in Appendix E, reveal Raman emission characteristic of the molecule. While the signals of the four lowest concentrations appear to overlap, the spectrum of the highest concentration (6.250 mM) of cholecalciferol solution throughout the region of interest shows a constant 1×10^5 counts higher than the others. This is possibly due to a difference in the position of the cuvette. Independent of this, there do appear to be regions in which cholecalciferol produced Raman emission, such as near 333 and 1100 cm^{-1}, but most notably at 1650 cm^{-1}. Cholecalciferol clearly possesses vibrational modes that produce Raman emission, but, once again, no fluorescence is apparent.

Melanin

Melanin was found to be the first of the selected samples to exert significant fluorescence as a result of NIR excitation. The spectra of melanin at various concentrations relative to the stock solution are depicted in Figure 11. From the raw data, it can be seen that each melanin sample follows the general trend and shape of the signal produced by water, much as was observed for the other water-soluble antioxidants. However, unlike the water soluble antioxidants, there is significant signal in addition to that of water, which is most apparent in the baseline subtracted spectra. Rather than displaying peaks of energies of limited

range, which is the case for emission by Raman scattering, this emission is across the entire 300-1900 cm^{-1} region of the spectrum. The strongest fluorescence emission is located in the middle of the region (600-1000 cm^{-1}) and slopes downward towards both higher and lower energies. This broad feature, consistently produced, can be a result only of melanin fluorescence.

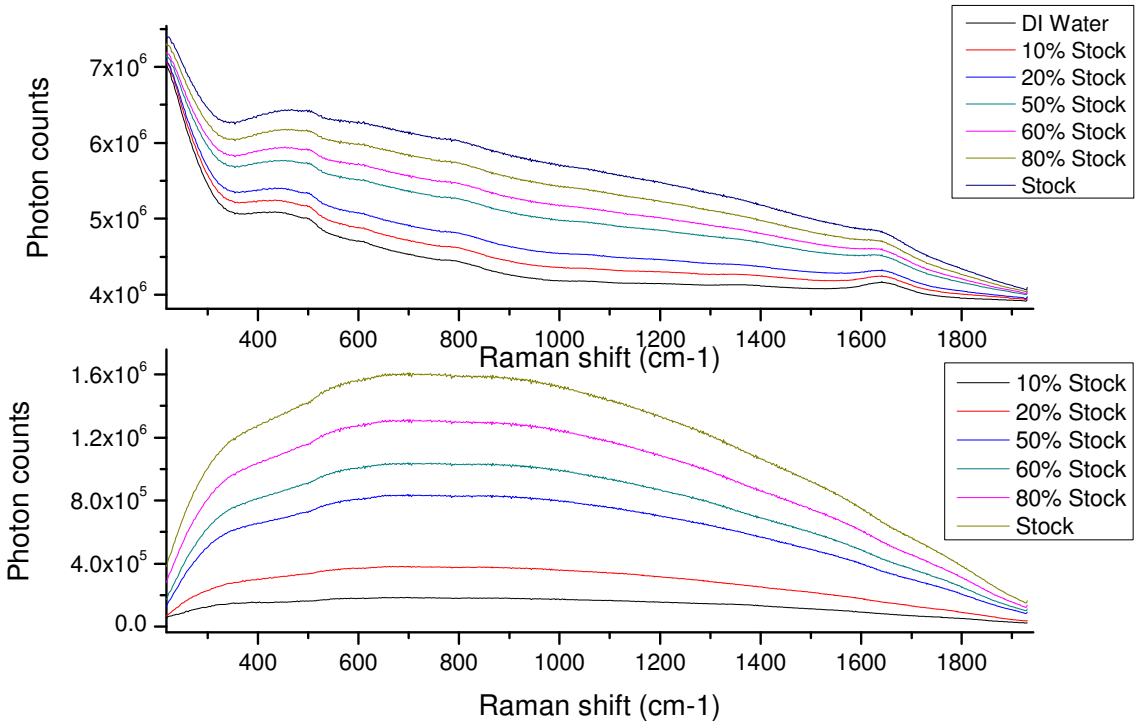

Figure 11: Raw non-subtracted (top) and subtracted (bottom) spectra of melanin in deionized water at varying concentrations. Because significant mass did not dissolve, absolute concentrations could not be determined, and relative concentrations are instead shown. Strong fluorescence that increases with concentration is evident across nearly the entire region.

Not only is it evident from these spectra that melanin fluoresces, but also it is apparent that there is a direct relationship between the overall fluorescence and the concentration of melanin, with striking linearity. The

integral of the region across which the melanin fluoresces was set as a function of concentration, yielding the plot displayed in Figure 12. The linear regression (R^2=0.998) serves as an effective model for the relationship between fluorescence and the concentration of melanin.

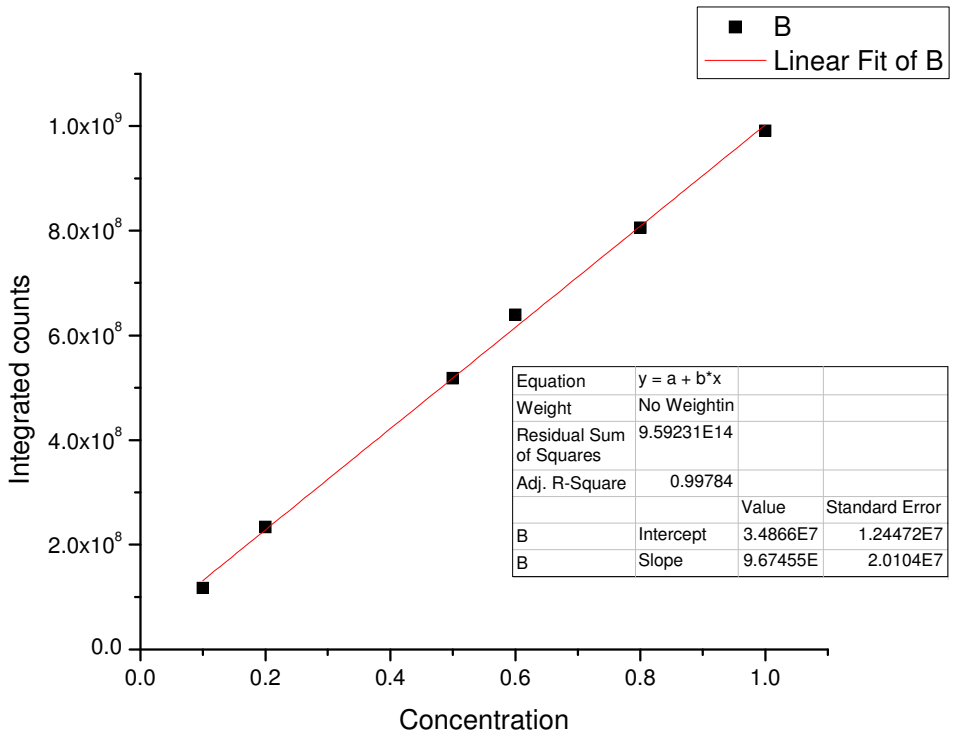

Figure 12: Integral of fluorescence as a function of relative concentration. Integration of melanin spectra was performed across the region 220-1928 cm^{-1}, the region displayed in Figure 11. Linear fit was applied, and statistics on fit are displayed.

Once it was identified that melanin does in fact fluoresce (the magnitude of which depends on its concentration in solution), the subsequent experiments assessing photobleaching and recovery were performed yielding the plot shown in Figure 13. From the fluorescence vs. time curve labeled “bleaching process,” it is clear that the fluorescence of melanin decreases over time. There was a sharp decrease in fluorescence

over the first ten minutes and then the slope evened out, as the fluorescence decayed at a relatively constant rate for the remainder of the experiment. The fact that the fluorescence decreased from 6.45×10^6 to 4.7×10^6 integrated counts represents a 27.1% decrease in signal over 60 minutes.

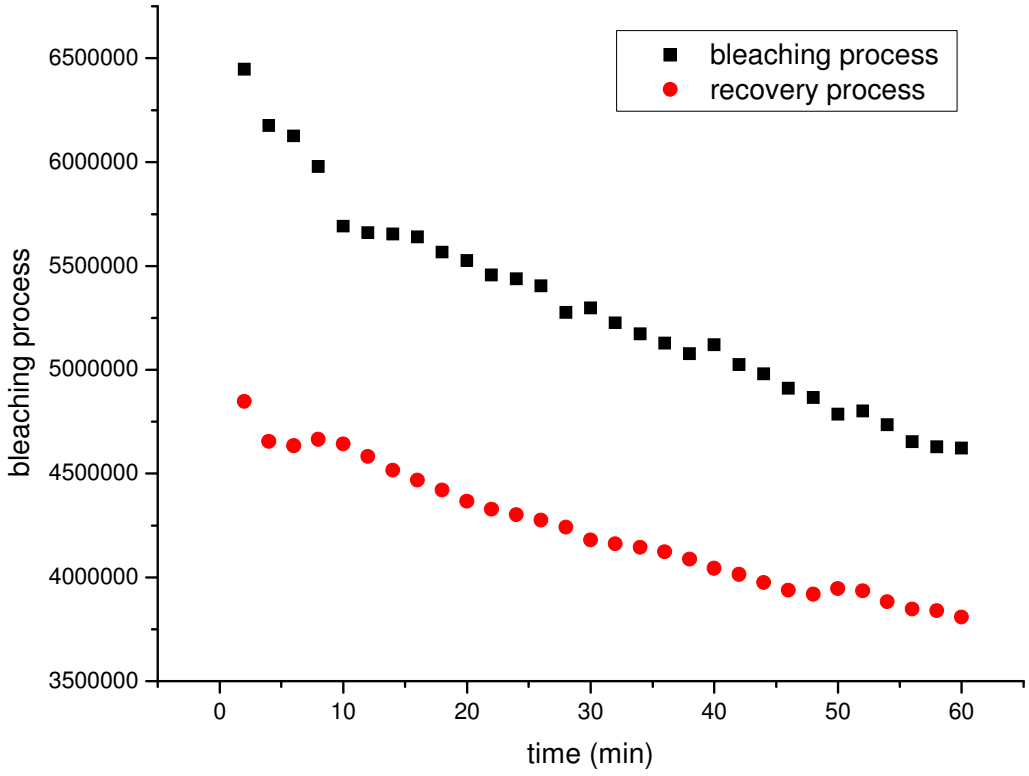

Figure 13: Graphs for integrated fluorescence as a function of time for two separate experiments: the first representing a typical experiment measuring changes in fluorescence over time (labeled bleaching process), and the second representing an identical experiment following a 2-hour delay, during which the sample was left motionless, in the dark, and unexposed to the laser. An experiment allowing 12-hour delay produced a similar result.

Following the 2 hours allowing the melanin to recover its fluorescence, the fluorescence vs. time curve labeled “recovery process” in Figure 13 revealed that melanin might recover fluorescence to a very

small degree. It appears there might have been a slight recovery, as the fluorescence of the point at t=2 min was approximately 4.85×10^6 integrated counts, an increase of 3.2% from the final value of 4.7×10^6 integrated counts from the bleaching process curve. This short, sharp decrease in fluorescence was followed by a steady decay that continued for the duration of the experiment. Also, from this curve it is clear that using the laser excitation of 785 nm at 450 mW, a fresh melanin solution does not fully photobleach after 60 minutes, for there is an additional decrease of 13.9% in fluorescence from the original fluorescence of 6.45×10^6 counts. With two hours of laser exposure, combined with no significant recovery during the 2 hour gap, it is possible that melanin may continue to decrease in fluorescence beyond this time span.

Discussion

All tissues in an organism are under oncotic pressure, a type of osmotic pressure that exists across physiological compartments as a result of electrostatic gradients, the pressure exerted within the circulatory system, and hydrostatic pressure as a result of gravity[20]. Given these conditions, this study sought to determine the timescale of possible fluid equilibration due to changing body posture, defined as hydrostatic relaxation, while in contact with the LighTouch® device.

Using the red blood cell data plotted by an integration of the Raleigh line, it is clear that the volume fraction of RBCs remained relatively constant during each of the three trials. Also, it appears that the

RBC volume fraction was nearly identical for trials A and B, but was significantly higher for trial C. Given that the overall integrated fluorescence (BV) of C is higher than that of both A and B, this would corroborate with the notion that elastic emission decreases as RBC concentration increases. Therefore, it appears likely that there was more blood present in the irradiated volume for measurement C than for measurements A and B, which likely was a result of the hydrostatic relaxation exercises which were intended to re-equilibrate and redistribute fluids.

According to Figure 5, while the volume fraction of RBCs remained were nearly the same and remained constant throughout A and B, the same blood did not remain in the irradiated area throughout the course of the two trials. Blood circulates, and oxygenated blood replaces deoxygenated blood to maintain the oxygen supply to all cells. Therefore, over the course of A and B, there was no net change in blood volume. Both the RBC and BV data show evidence of pulsing throughout each of trials A, B and C. It appears that, since B immediately succeeded A, any photobleaching of tissue occurred over the course of A, for any decrease in fluorescence during B was insignificant compared to the decay observed in A.

This evidence is complemented by the results obtained from the BV data from the fluorescence recovery experiment, depicted in Figure 6. Once it became clear that the laser had an effect on the tissue within the

irradiated volume, this experiment was designed to probe how long and to what degree the tissue could recover its fluorescent properties after being exposed to NIR light for a period of time. It became evident that, because fresh blood had certainly been circulated through the irradiated volume, the chemical changes induced by the laser are not appreciably reversed when laser exposure is terminated over the period of time that blood is replenished.

If blood were the species that was being photobleached, the photobleached blood would be replaced by fresh non-photobleached blood, and the overall fluorescence would have remained high over the course of any typical experiment, instead of exhibiting a continuous decrease. Given the time to fully ensure the blood had circulated for measurement B, the lack of significant recovery of fluorescence, after blocking the laser, supports the idea that a substance other than blood must photobleach. It is clear that the presence of the laser upon the exposed tissue is solely responsible for the photobleaching effect, and differences in hydrostatic pressure seem to have little impact. Since the decay is still quite evident even when fresh blood is always being circulated, it is apparent that the species responsible for the photobleaching effect is not contained within blood, but within the static tissues.

From these experiments, it has been shown that a substantial fraction of the decay in fluorescence is not a result of blood movement, but

instead is the result of a change in the fluorescent properties of the static tissues. Fluorescence regularly decays from 15-20%, and even up to 33%, depending on the individual. This change in fluorescence, which is not a result of blood movement, severely challenges the accuracy of the noninvasive *in vivo* determination of blood glucose concentration, because the model for achieving this depends on the assumption that a change in fluorescence represents a change in blood volume. These data suggest that a “pre-bleaching” phase is advisable, in which time is allowed for the finger to be exposed to the laser so that any photobleaching of the static tissues may occur. This seems to be a relatively effective technique that has been experimentally shown to reduce the effect of photobleaching and to improve blood glucose measurements. These results also prompted the *in vitro* experiments to ascertain which substances in static tissue undergo a chemical change into products that are less fluorescent.

While it was originally hypothesized that several of the most common antioxidants might fluoresce as a result of NIR excitation, it became clear that this is not the case. In summary, not one of the six antioxidants studied fluoresce as a result of near-infrared excitation. Antioxidants do possess loosely held electrons that are essential to their function to sequester reactive oxygen species[6], but it appears that an excitation by a photon in the NIR region does not provide enough energy to promote them to an excited quantum state such that the molecule could exhibit subsequent fluorescence. While it does seem that each of these

substances do undergo Raman scattering, producing emission characteristic of their structures, the emission of these compounds at their physiological concentrations both individually and collectively is far too weak to be responsible for the photobleaching that causes a decay of up to 33.7% of the original fluorescence signal.

Since there is very little literature regarding Raman spectroscopy and these substances, these findings serve an important purpose. There are innumerable substances in blood and in static tissue, so it is extremely difficult to isolate those which contribute to the fluorescence observed from the tissue of the volar side of fingertips. As previously stated, it is vital to the use of Raman spectroscopy to determine blood glucose concentration that the assumption that fluorescence is associated with blood volume, and specifically that any changes in fluorescence are a result of movement of blood, remains true. Since the photobleaching of static tissue weakens the merit of this premise, it is clearly necessary to determine which substances do, in fact, contribute to the regular decay of at least 15-20% of the total fluorescence signal. It is also useful, however, to identify the substances that do not fluoresce nor photobleach. Narrowing down the list of potential candidates, and learning more about specific Raman characteristics of certain compounds, are important to the overall effort to recognize the contribution of substances to tissue fluorescence.

The *in vitro* studies of melanin reveal that it fluoresces as a result of

NIR excitation and does so linearly as a function of concentration. The fact that the fluorescence of melanin decreases as exposure is prolonged strongly suggests that it undergoes a laser-induced chemical change to a less fluorescent form. It has been observed that the oxidation state of melanin affects its UV-Vis emission[24]. While it is believed that these are the first reports of NIR-excited emission spectra of melanin, the oxidation state may also be a factor in its fluorescence as a result of NIR excitation. The relatively small recovery by melanin, which is similar to what is observed *in vivo*, means that melanin, as it exists in skin, could possibly contribute to the photobleaching of tissues and interfere with the ability to accurately determine blood glucose concentration.

It must be noted that the synthesized eumelanin studied using spectroscopy *in vitro* is very different from melanin *in vivo*. Melanin, which functions as a skin pigment, is located throughout cells called melanocytes. In these cells, the structure of melanin is of a very complex nature, and can vary among individuals. These differences in structure are compounded by mechanisms that ultimately result in varying skin tones. There are many proposed models that predict a possible structure of melanin as it exists *in vivo*, but these are yet to be verified[7]. To reproduce melanin as it exists in the tissue of the volar side of human fingertips is a very difficult task. It was originally found that melanin was virtually insoluble in water, but in this study, as time progressed, observations of the solution one week, one month, and four months after the creation of

the solution revealed that melanin was slowly becoming increasingly soluble in water. What started as a dark, brownish-black suspension eventually yielded a yellowish-brown supernatant.

It is believed that over time, the melanin polymer was degraded, and the large water-insoluble particles were divided into much smaller ones, likely by hydrolysis, which were in fact soluble. These did not cause any loss of signal by scattering as a result of the turbidity of the solution. Due to the fact that this color was the darkest, and remained visible after even a four-month period, and to the fact that skin color can be much darker, it is inferred that *in vitro* melanin may not be a complete representation of melanin *in vivo*. Given that melanin's structure is complex, and that the skin of the volar side of fingertips contain far fewer melanocytes than skin of the dorsal side, it remains difficult to quantify melanin's contribution to the photobleaching of static tissue. Therefore, it is believed that the photobleaching of melanin must be only a relatively small contribution to the decay in fluorescence observed in static tissue.

Conclusion

It has been shown by various *in vivo* experiments that photobleaching of the static tissues occurs as a result of NIR laser exposure. Recovery by hydrostatic relaxation and the lack of recovery of fluorescence during an appropriate timescale indicate that the decay of fluorescence by the volar side of fingertips commonly originates not from the blood, but from the static tissues. While none of the antioxidants

studied were observed to fluoresce and photobleach as a result of NIR excitation, melanin was shown to exhibit these effects, indicating it could be a possible contributor to the overall photobleaching, and providing insight into the light-induced chemistry that occurs as a substance is photobleached.

References

[1] American Diabetes Association. *Standards of medical care in diabetes*. Diabetes Care, 2008. Vol. 31. Suppl 1:S12–S54

[2] Benjamin, Evan M. *Self-Monitoring of Blood Glucose: The Basics*. *Clinical Diabetes,* 2002. Vol. 20(1): p. 45-47.

[3] Khalil, O.S., *Non-invasive glucose measurement technologies: an update from 1999 to the dawn of the new millennium*. Diabetes Technol Ther, 2004. Vol. 6(5): p. 660-97.

[4] Deng, B., Wright, C., Lewis-Clark, E., Shaheen, G., Geier R. and Chaiken, J.. *Direct noninvasive observation of near infrared photobleaching of autofluorescence in human volar side fingertips in vivo.* Proc. SPIE, 2010, Vol. 7560-24.

[5] Chaiken, J., et al. *Noninvasive in-vivo tissue-modulated near-infrared vibrational spectroscopic study of mobile and static tissues: blood chemistry*. Proc. SPIE, 2000, Vol. 3918: p. 135-143.

[6] Masaki, H. *Role of antioxidants in the skin: Anti-aging effects.* J. Dermatol. Sci, 2010. Vol. 58(2): p. 85-90. PMID: 20399614.

[7] Watt, A., J. Bothma, and P. Meredith. *The supramolecular structure of melanin.* Soft Matter. 2009. Vol. 5: 3754–3760.

[8] Blackwell, J., et al., *In vivo time-resolved autofluorescence measurements to test for glycation of human skin*. J Biomed Opt, 2008. Vol. 13(1): p. 014004.

[9] McCreery, R.L.. *Raman Spectroscopy for Chemical Analysis*. Volume 157 in Chemical Analysis: A Series of Monographs on Analytical Chemistry and Its Applications. Ed. Wineforderner, J.D. New York: John Wiley & Sons Inc., 2000, p. 2-20.

[10] Smith, Ewen, and Geoffrey Dent. *Modern Raman spectroscopy: a practical approach*. 1st Ed. Chichester, England: John Wiley & Sons Ltd., 2005.
p. 1-20.

[11] Tinoco, I., et al. *Phyiscal Chemistry: Principles and Applications in Biological Sciences*. 4th ed. Upper Saddle River, New Jersey: Prentice Hall, 2002. 554-579.

[12] Chaiken, J., et al. *Noninvasive blood analysis by tissue modulated NIR Raman spectroscopy*. Proc. SPIE, 2001, Vol. 4368, 134-145.

[13] Chaiken, J., et al. *Noninvasive, in-vivo, near infrared vibrational spectroscopic study of lipid and aqueous phases of skin and near surface tissues*. Proc. SPIE, 2000, Vol. 3907, 89-97.

[14] Chaiken, J., et al., *Effect of hemoglobin concentration variation on the accuracy and precision of glucose analysis using tissue modulated, noninvasive, in vivo Raman spectroscopy of human blood: a small clinical study*. J. Biomed. Opt., 2005. Vol. 10(3): p. 031111.

[15] Chaiken, J., et al., *Simultaneous, noninvasive observation of elastic scattering, fluorescence and inelastic scattering as a monitor of blood flow and hematocrit in human fingertip capillary beds*. J. Biomed. Opt., 2009. Vol. 14(5): p. 050505.

[16] Berg, Jeremy M., John L. Tymoczko, and Lubert Stryer. *Biochemistry*. 6th ed. New York: W.H. Freeman and Company, 2007. 577-585.

[17] Dyer, D.G, Blackledge, J.A., Thorpe, S.R., and Baynes, J.W. *Formation of Pentosidine during Nonenzymatic Browning of Proteins by Glucose*. Journal of Biological Chemistry, 1991. Vol. 256(18). p. 11654-11660.

[18] Chaiken, J., et al. *Instrument for near infrared emission spectroscopic probing of human fingertips in vivo*. Review of Scientific Instruments 81, 034301, 2010.

[19] Chaiken, J., et al. *Noninvasive in vivo tissue and pulse modulated Raman spectroscopy of human capillary blood and plasma*. Proc. SPIE, 2006, Vol 6093, 609305-1.

[20] Leyk, D., Eßfeld, D., Baum, K., & Stegemann, J. *Influence of the gravity vector on early time courses of leg blood flow during calf exercise.* Proceedings 5th Eur. Symp. on 'Life Sciences Research in Space'. 1994. ESA SP-366: 275-279.

[21] Saxena, T., Chaiken, J., et al. *Near Infrared Raman Spectroscopic Study of Reactive Gliosis and the Glial Scar in Injured Rat Spinal Cords.* Proc. SPIE, 2009, Vol. 7560-23.

[22] Lentner, C., *Geigy Scientific Tables Vol. 3: Physical Chemistry, Composition of Blood, Hematology, Somatometric Data*. 8th ed. Geigy Scientific Tables. Vol. 3. 1984, West Caldwell, NJ: CIBA-GEIGY.

[23] Tschirner N., Schenderlein M., Brose K., Schlodder E., Mroginski M.A., Thomsen C., Hildebrandt P.. *Resonance Raman spectra of beta-carotene in solution and in photosystems revisited: an experimental and theoretical study.* Physical chemistry chemical physics, 2009. Vol. 11(48):11471-8 PMID: 20024418.

[24] Kayatz, P., et al., *Oxidation causes melanin fluorescence*. Invest Ophthalmol Vis Sci, 2001. Vol. 42(1): p. 241-6.

Appendices

Appendix A: Plot of integrated signal from 1475-1650 cm^{-1} of beta carotene, and linear fit applied indicating dependence of signal strength on concentration.

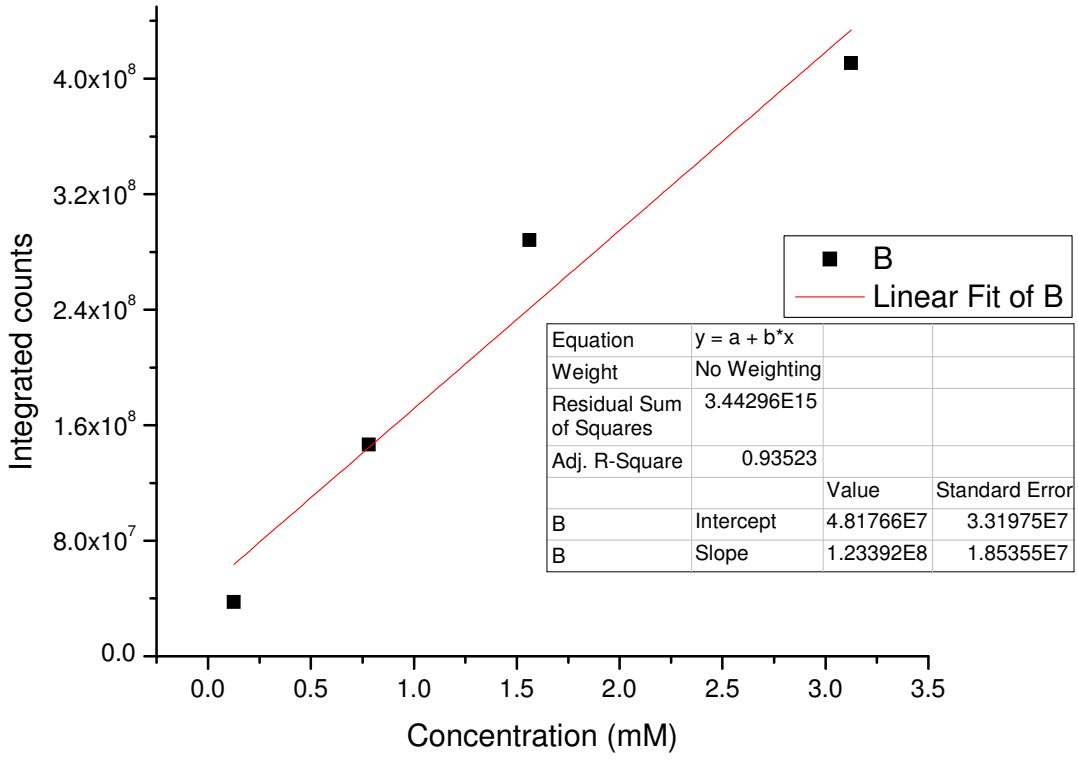

Appendix B: Subtracted (top) and raw non-subtracted (bottom) spectra of reduced glutathione in cyclohexane at varying concentrations.

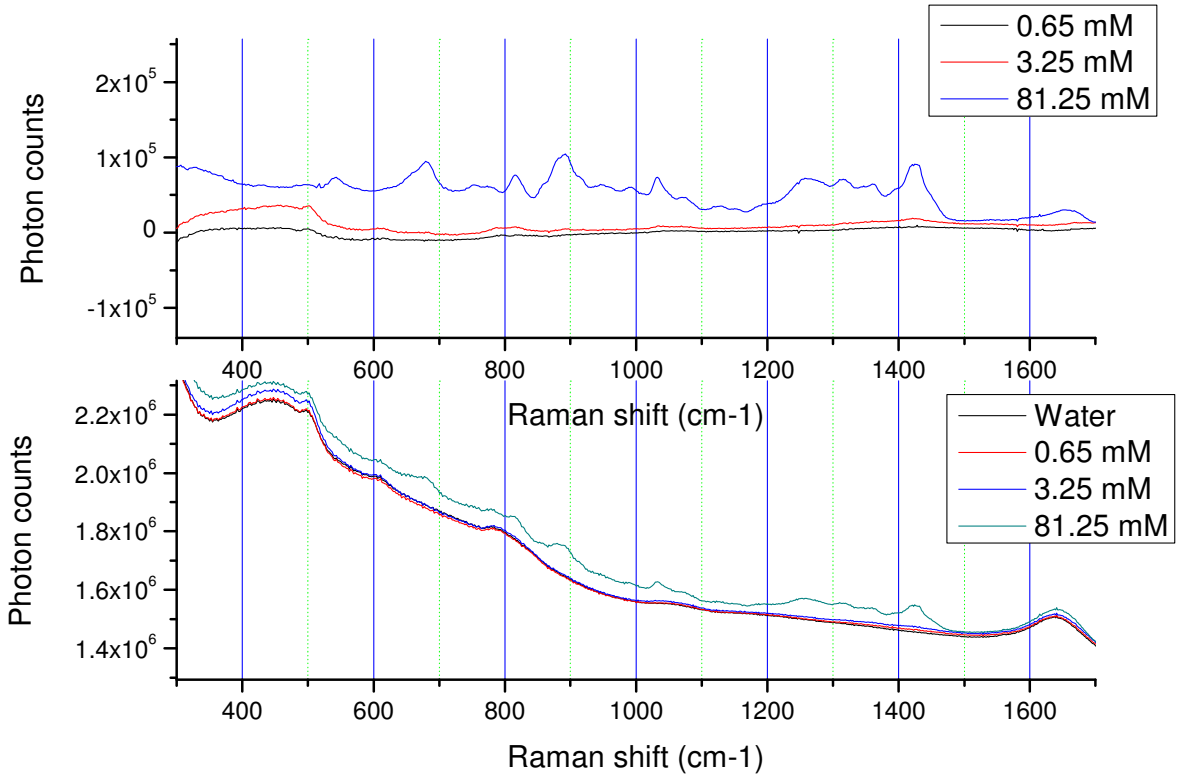

Appendix C: Subtracted (top) and raw non-subtracted (bottom) spectra of uric acid in cyclohexane at varying concentrations.

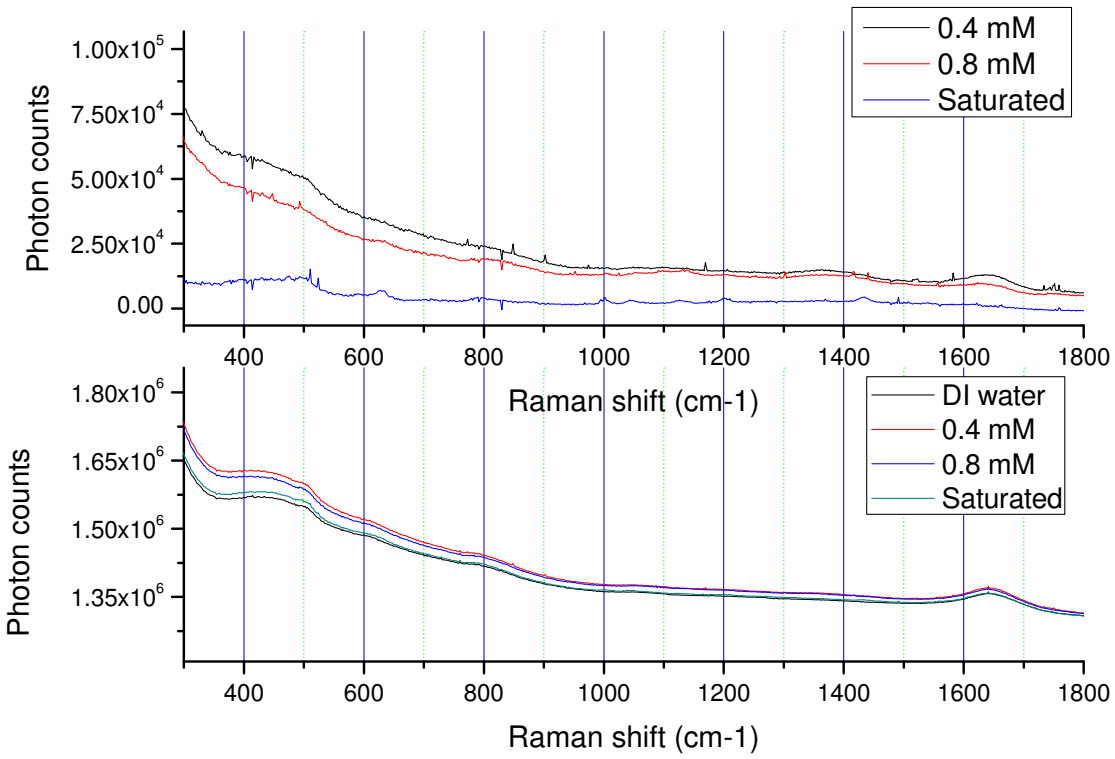

Appendix D: Raw non-subtracted (bottom) spectra of ±-α-tocopherol at varying concentrations. Cyclohexane baseline subtraction did not occur cleanly, and therefore, only raw data is shown.

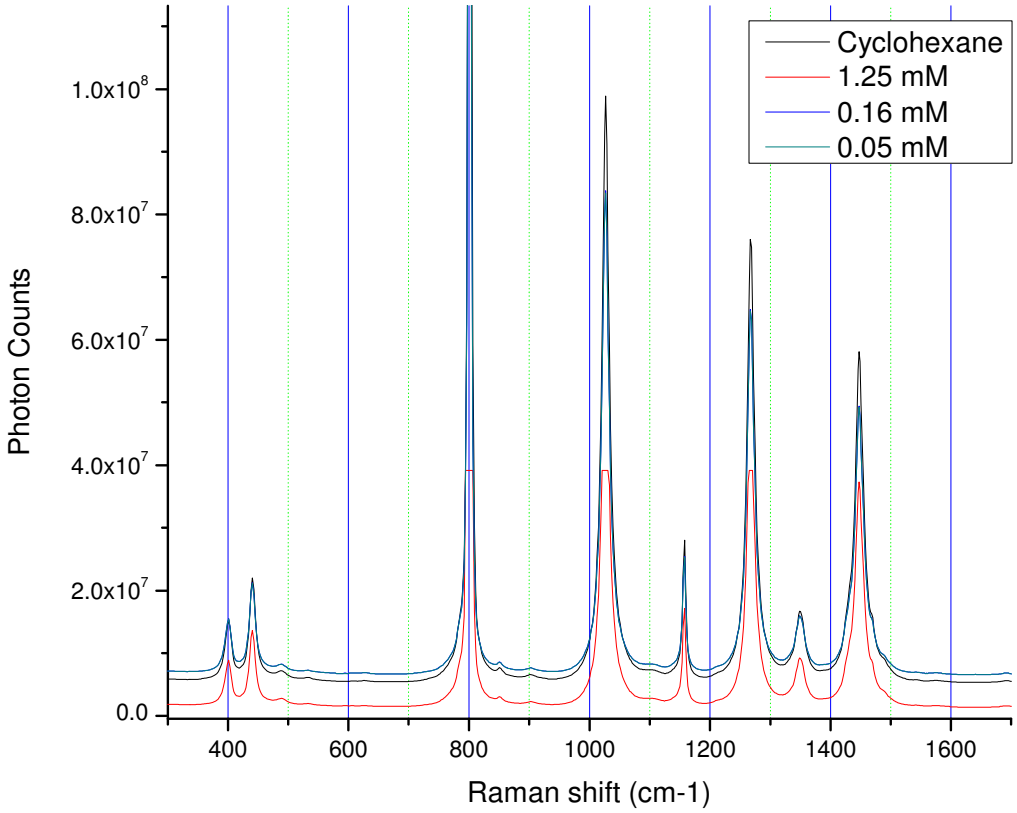

Appendix E: Raw non-subtracted (bottom) spectra of cholecalciferol at varying concentrations. Cyclohexane baseline subtraction did not occur cleanly, and therefore only raw data are shown. The tops of the major peaks (due to cyclohexane) extend to nearly 4×10^7 counts.

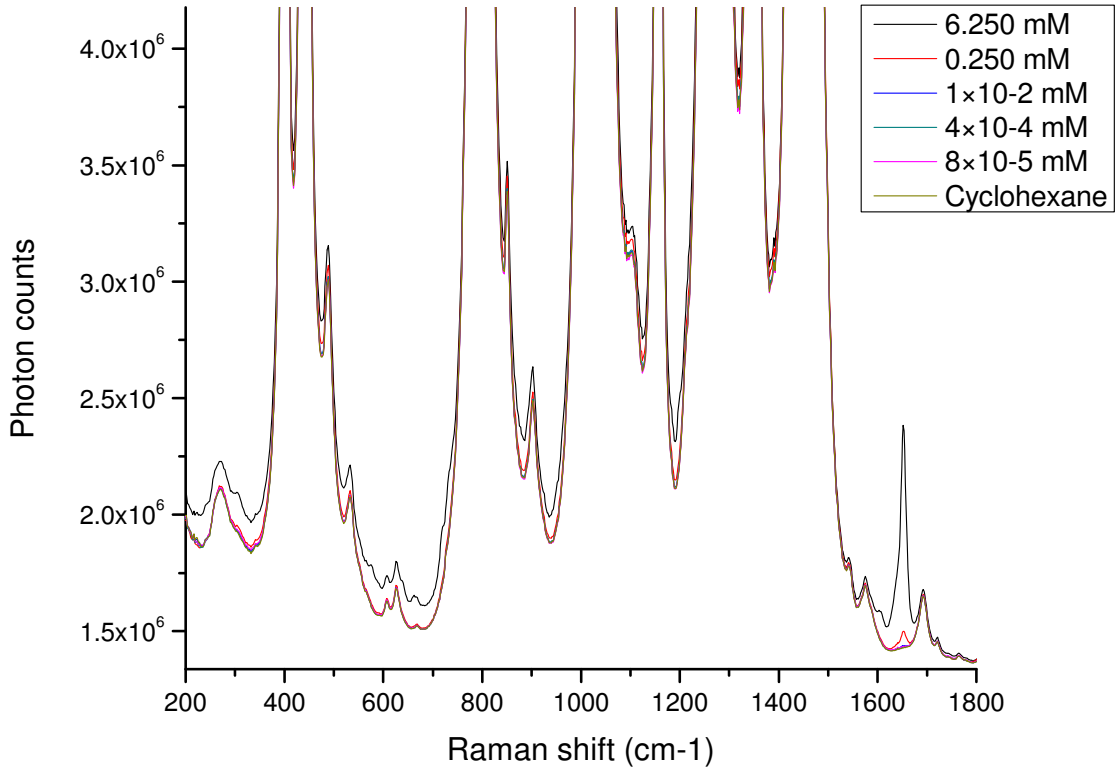

Capstone Summary

Diabetes mellitus affects millions of Americans and is one of the most difficult conditions to manage. Characterized an inability maintain a healthy blood glucose concentration, diabetes, if not properly handled, can be potentially be fatal, as well as cause blindness, cardiovascular disease, and foot ulceration. To ensure their blood sugar is at a healthy balance, diabetes patients must monitor their blood glucose concentration several times each day. The current commercial technology requires the invasive procedure of extracting a sample of blood to determine their blood sugar level, and diabetics must suffer from scarred and tender fingers. Our technology at LighTouch Medical implementing Raman spectroscopy to noninvasively determine blood glucose concentration *in vivo* may someday relieve the pain of diabetes management, as well as provide additional information about blood such as hematocrit.

The concentration of a particular substance is defined as an amount per unit volume of that substance. Blood volume and the relative glucose content of that blood volume can both be associated with certain features of an emission spectrum of the volar (palmar) side of human fingertips, allowing for the determination of blood glucose. When a monochromatic laser in the near-infrared region of the spectrum 785 nm is shined onto a sample, molecule-light interactions occur. The photons of different wavelengths are quantified by a detector and processed by a computer to yield an emission spectrum. There are two devices that are available for

experimentation consisting of virtually the same optical layout, involving a laser, a detector, and various filters and lenses. The first allows for the study of solid and liquid samples, and the second, the LighTouch® device, is customized for the analysis of human fingertips.

The emission produced reflects upon specific interactions between molecules and photons. Light can be scattered, in which a photon briefly perturbs the electron cloud surrounding the molecule and is then reflected into a different direction. In most cases, the photon is reflected at the same energy upon incidence, called Raleigh scattering, but based on structural features and vibrational modes of the molecule, the photon may be reflected at a different energy (higher or lower) than then the incident photon, a weaker process known as Raman scattering. Light can also be absorbed by molecules, promoting the molecule to an excited electronic state, if so, upon relaxation to the ground state, there will be an emission of a photon, a process called fluorescence. Raman scattering is typified on an emission spectrum by sharp narrow peaks, while fluorescence is observed as a broad feature spanning over a wide range of energies. It has been previously discovered that red blood cell volume can be associated with Raleigh scattering, presence of glucose with a specific Raman feature, and blood volume with fluorescence.

The integration of fluorescence is used to monitor blood volume (BV) over the course of experiments, and the integration of the Raleigh line for red blood cell content (RBC). For virtually all experiments, a

decline has been observed over the course of experiments until a steady state is reached. One of the most important assumptions in our theory behind the association of blood volume with fluorescence is that changes in fluorescence are the result of blood movement. It was hypothesized that blood volume was not the cause of the decay in fluorescence. To investigate further, a series of experiments were performed.

First, because circulation of blood is so complex and depends on a number of factors, three scans, measuring BV and RBCs, were performed to ascertain the effect of hydrostatic relaxation (the process of achieving fluid equilibration by stretching, muscle contraction/relaxation, etc.) on the effect of fluorescence. The first scan was taken place after hydrostatic relaxation exercises (A), the second was taken ten seconds after the first experiment while the hand remained motionless to allow fresh blood to circulate (B), and the third was taken following additional hydrostatic relaxation and the finger placed in a slightly different position (C).

The BV curve for A demonstrated the decay in fluorescence until the steady state was reached. The BV curve for B maintained approximately the same steady state that was reached in A, and the curve for C resembled that of A. The RBC measure of A and B were nearly identical. Due to the fact that the BV curve of B was at the same level reached at the end of A, even though blood had circulated, it is determined that the decay in fluorescence must not be a result of movement of or change in fluorescent properties of blood. An additional experiment which

demonstrated that there is little recovery of fluorescence over a dozen cardiac pulses after photobleaching corroborated these results. It was ultimately concluded that the source of the decay in fluorescence was laser-induced chemistry, a process known as photobleaching, within static tissue.

Antioxidants serve to protect essential cellular molecules from rapid oxidation by reactive oxygen species by themselves undergoing oxidation[6]. Since antioxidants contain loosely held electrons, which are essential to their function as reducing agents of reactive oxygen species, it was hypothesized might fluoresce and photobleach. Melanin has high absorptive properties, rendering it ideal as a skin pigment. With such high absorptivity, melanin became a candidate of interest as to its fluorescent and photobleaching properties as well.

Solutions were made at different concentrations of melanin and the following six antioxidants: L-glutathione, uric acid, β-carotene, cholecalciferol, L-ascorbic acid and ±-α-tocopherol. To overcome differences in solubility, some antioxidants were dissolved in cyclohexane, and the others in deionized water. Melanin was allowed to rest in deionized water for four months so that the polymer would break down into smaller soluble particles. These solutions were scanned using the *in vitro* Raman instrument. Ultimately, it was determined that none of the antioxidants exhibited any fluorescence. Melanin, however, did fluoresce in a manner than increased directly and linearly with concentration.

Given that melanin appeared to fluoresce, additional experiments were performed to determine whether or not it photobleaches, and if so, recovers its fluorescent properties over time. While melanin was exposed to the laser, overall fluorescence was measured over short intervals. It was observed that melanin did photobleach, and after leaving the melanin motionless in the dark for two hours, by the same process, it was determined that it did not substantially recover its fluorescent properties.

While the hypothesis that these antioxidants might fluoresce was disproven, there was much learned by ruling out the possibility that several substances are involved in the photobleaching of skin tissue. There are innumerable substances in blood and in static tissue, and since there is very little literature regarding the NIR Raman emission of these substances, it is extremely difficult to isolate those which contribute to the fluorescence observed from the tissue of the volar side of fingertips. It was an essential first step towards sorting out which compounds do and do not fluoresce, so that the problem of photobleaching can be properly addressed.

The revelation of melanin's fluorescence and photobleaching provides an insight into the processes that account for photobleaching of static tissue. Since melanin (contained in specialized pigment cells called melanocytes) is relatively scarce on the volar side of fingertips, it is not likely the prominent source of fluorescence and photobleaching. These results, however, along with its complex structure which has yet to be

elucidated, arise many interesting questions.

Many factors, including the macromolecular structure, the oxidation state, and its interaction with other biological molecules, are likely involved with the fluorescence and photobleaching processes. These results prompt further investigation as to the chemistry of melanin's photobleaching. Should this become clear, a greater understanding as to the photobleaching of more prominent substances in the volar side of human fingertips may be achieved, so that they may be appropriately accounted for (such as by a pre-bleaching phase) to improve the accuracy of the noninvasive *in vivo* blood glucose monitor.